PRELIMINARY REPORT OF THE CHARMO (JARMO) PREHISTORIC INVESTIGATIONS, 2023

Akira TSUNEKI[*1], Saber Ahmed SABER[*2], Nobuya WATANABE[*3], Ryo ANMA[*4], Sari JAMMO[*5], Mariko MAKINO[*6], Yuko MIYAUCHI[*7], Kirsi O. LORENTZ[*8], Yu ITAHASHI[*9], Minoru YONEDA[*10], Masanori KUROSAWA[*11] and Kei IKEHATA[*12]

1. Introduction

The team of the University of Tsukuba aimed to understand the Neolithization process in the Near East and advance archaeological investigations in the eastern wing of the Fertile Crescent a step forward. Slemani is not only located at the heart of the eastern wing of the Fertile Crescent but also in the area where the study of Neolithization was initiated in the 1940s. Fortunately, with the great help and permission of the Directorate of Antiquities of the KRG, the University of Tsukuba team started investigating Neolithization in this area in 2014. Excavations were undertaken at Qalat Said Ahmadan (2014, 2015) [Tsuneki *et al*. 2015, 2016] in the Raparin area, in addition to surveys at Charmo (Jarmo) and Turkaka (2016–2018) [Tsuneki *et al*. 2019] in the Chamchamal area.

The results of the excavations at Qalat Said Ahmadan were fruitful. We discovered an intermittent cultural sequence, ranging from the late phase of the Pre-Pottery Neolithic (middle of the 8th millennium) to the Ubaid period. However, this sequence does not appear to include the earliest Neolithic deposits. The Neolithic cultural sequence discovered in Shimshara [Mortensen 1970] on the Raniya Plain in the Raparin area appears to be almost the same as that of Qalat Said Ahmadan. We do not know whether the Raparin area lacks the earliest Neolithic deposits or whether these sites lack the deposits of that period. Therefore, since 2016, we have explored Neolithization in the Chamchamal area as well.

To develop a more complete scheme of the Neolithization process, we must understand the long cultural sequence from the Epi-Paleolithic to the Pottery Neolithic periods. In the Chamchamal area of the Zagros region, research by the University of Chicago revealed the proximity of Cham Gawar, Turkaka, a terminal Paleolithic site; Karim Shahir, a transitional site from the Paleolithic to the Neolithic; and Charmo, an early Neolithic site (Figs. 1-1, 1-2). These are considered a crucial group of sites for discussing the Neolithization of the Zagros region. In recent years, they have been reexamined by the UCL at Charmo (Fuller 2015, Carretero *et al*. 2023) and by the University of Liverpool at Karim Shahir. We believe that further investigation of these sites and landscapes from new perspectives and using technologies will further our understanding of the Neolithization process in the Zagros region. Therefore, we had a strong motivation to re-examine these sites from a new perspectives and use novel techniques.

*1 Professor Emeritus, University of Tsukuba
*2 Researcher, Directorate of Slemani Antiquities and Heritage, KRG, Iraq
*3 Professor, International Digital Earth Applied Science Research Center, Chubu University
*4 Professor, Graduate School of Technology, Industrial and Social Sciences, Tokushima University
*5 Researcher, Research Center for West Asian Civilization, University of Tsukuba
*6 Assistant Professor, Research Institute of Cultural Properties, Teikyo University.
*7 Ph.D. candidate, Science and Technology in Archaeology and Culture Research Center, The Cyprus Institute
*8 Associate Professor, Science and Technology in Archaeology and Culture Research Center, The Cyprus Institute
*9 Associate Professor, Institute of Humanities and Social Sciences, University of Tsukuba
*10 Professor, The University Museum, The University of Tokyo
*11 Associate Professor, Faculty of Life and Environmental Sciences, University of Tsukuba
*12 Associate Professor, Faculty of Life and Environmental Sciences, University of Tsukuba

Fig. 1-1 Three prehistoric sites along the Cham Gawra.

Fig. 1-2 UAV photo of Charmo, Turkaka and Karim Shahir.

With the kind permission of the Directorate of Antiquity and Heritage of the KRG, we executed the measurement survey at Charmo in the summer of 2016 and created a detailed map and 3D images using GPS and UAV (Fig. 1-3).

In 2017, we conducted extensive GPS and unmanned aerial vehicle (UAV) surveys and created a detailed map covering Turkaka and Charmo. We also created small-sounding trenches at Turkaka and identified the age and characteristics of the sites. The cultural layers are very thin (~0.5 m) and no definite architectural remains have been discovered. Two suitable datings of ^{14}C indicate that the site was used repeatedly and briefly during *c*. 18,500–16,500 cal. BC. The results of the sounding excavations and inventory of chipped stones indicate that prehistoric people used the Turkaka site as a place to produce chipped stones, especially blades and micro-blades, during the Zarzian period, much before the Proto-Neolithic period. Thus, Turkaka is clearly a Pre-Neolithic site and not directly related to neolithization. However, importantly, the Charmo-Turkaka-Karim Shahir

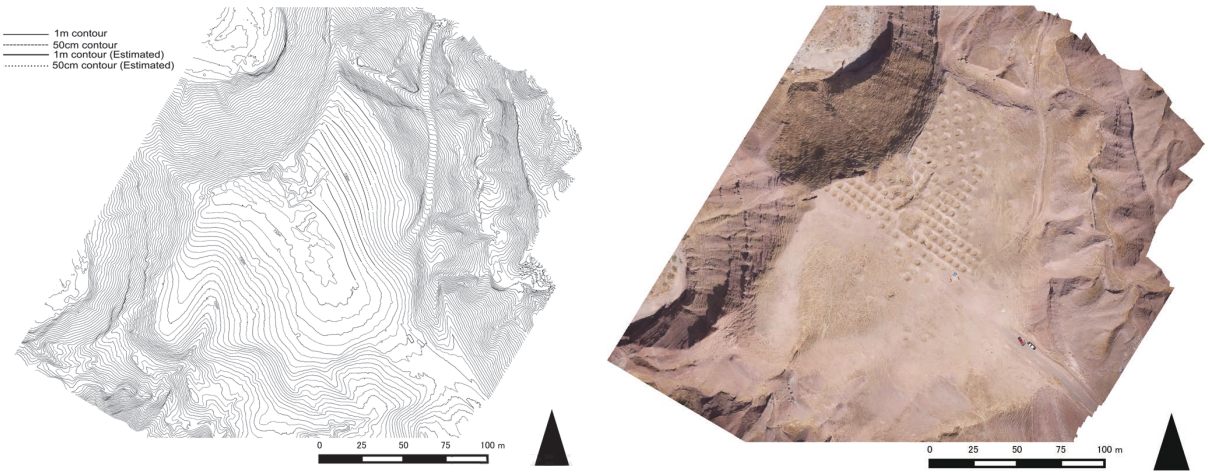

Fig. 1-3 Topographic map and orthographic image of Charmo made using UAV (made by N. Watanabe).

share similar environmental characteristics of being located on a freshwater-rich hillside surrounded by the Cham Gawra, with an abundance of chert suitable for stone tool making, and springs from the sandstone-marlstone cuesta topography, which were critical factors in the neolithization of the Chamchamal area.

Owing to this in-depth knowledge of the location of the Chamchamal prehistoric sites, we determined that Charmo was located on an extremely prosperous freshwater land. This environment affected the formation of early farming villages in this area. Therefore, we decided to concentrate our research on Charmo to explain the neolithization process in this area.

During the 2018 season, we continued our measurement surveys at Charmo on a larger scale, particularly from the perspective of a series of springs. We also created small soundings in three locations at Charmo to detect cultural conditions for further investigation. These investigations revealed that Charmo was managed under extremely fruitful natural conditions. To the south of Charmo, the underflow water from the Zagros Mountains is gushed out by dozens or even several hundred meters. A series of *kani* (*Kani* is a spring in Kurdish) ranges in a few lines on a gentle slope, and they seem to irrigate the gentle slope land naturally toward the southwest from the northeast (Fig. 1-4). Accordingly, it is necessary to reconsider the preconception of primitive farming in the Zagros region as "simple rain-fed farming along the hilly flanks," as proposed by Robert Braidwood [Braidwood 1967]. We must add new perspectives and the concept of "more complicated farming using springs in the water reservoir area" to further understand the farming practices of the early Charmo people.

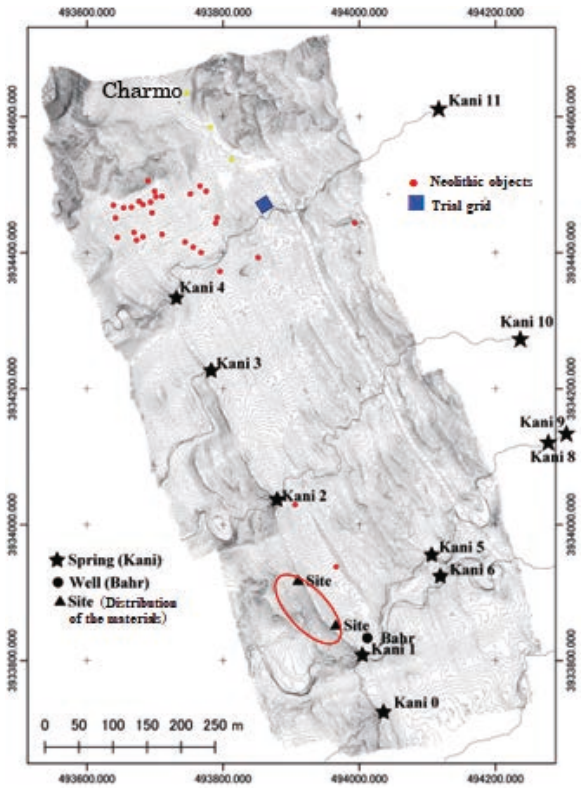

Fig. 1-4 Topographic map south of Charmo. Numerous springs (*kani*) exist to the south of the Charmo site.

Therefore, we decided to conduct our investigations at Charmo and hope to reconsider the Charmo site and obtain a variety of materials to reconsider the beginning of farming way of life in the Zagros region. We are, therefore, very grateful that our survey application has once again been approved by the Directorate of Antiquities and Heritage of the KRG and that the Directorate of Slemani Antiquities and Heritage fully supports us. During the 2019 season, we conducted exploratory soundings at the Charmo site and explored the prehistoric fields in the modern wheat field area south of the site. We also continued our work to extend Charmo's topographic map. In the 2020 and 2021 seasons, when we were unable to send a mission team from Japan because of the COVID-19 pandemic, we asked the Slemani Department to continue with small soundings in Charmo.

Fortunately, after the COVID-19 pandemic has faded, the Directorate of Antiquities and Heritage of the KRG allowed us to resume full-scale research at Charmo in 2022. With the new perspectives and purposes described above, we decided to take up the challenge of investigation at Charmo again.

(Akira Tsuneki)

2. Excavations at Charmo, the 2023 season

Excavations in the previous season had two main purposes. The first purpose was to establish the chronology of the Charmo site and determine the date of the last phase of the Charmo village. The second purpose was to reveal people's lives in the Charmo Neolithic village by excavating a relatively wide trench. For the first purpose, we set up a JT square on top of the Charmo cultural deposits. The series of ^{14}C data obtained from the JT square indicated that the Charmo Neolithic village ended in the late 7th millennium BC. The upper four layers at JT square produced a great number of potsherds, and they are thought to be the oldest pottery in Zagros, typologically Proto-Hassuna, or earlier. More precisely, both in absolute and relative chronological terms, the demise of the village at Charmo in the late 7th millennium can almost certainly be established. The J-II central square investigation provided a glimpse into the aspects of village life in the Pre-Pottery Neolithic period, including houses, *tannor*, and other basic living infrastructure [See Tsuneki *et al*. 2023].

Based on these results, the 2023 season excavations had two main objectives. The first was to establish the chronology of the Charmo site from the Pre-Pottery Neolithic to the beginning of the Pottery Neolithic period. In particular, we aimed to determine when villages began to form in Charmo. For this, we had to dig down to the virgin soil at Charmo and collect a series of samples for ^{14}C dating from each layer to fix the absolute ages of the beginning of the Charmo settlement. As for the villages at Charmo, last season's excavations at the J-II central square yielded rich results; thus, we assumed that continuing the investigations at the J-II central square would be the most useful, especially for gaining a deeper understanding of the conditions of the older Pre-Pottery Neolithic villages.

J-II central square

The aim of the investigation in this excavation square was to explore the oldest cultural layers at Charmo. Braidwood's research showed that the oldest cultural layers of Charmo were only detected in a small part of Operation J-I and Step Trench J-A, with a few trenches reaching virgin soil [Braidwood *et al*. 1983]. This left it unclear when and how the first settlement at Charmo began operating. Therefore, we decided to dig further by cleaning Operation J-II, which was the widest and reached the most extensive and relatively oldest cultural layer excavated by Braidwood during the previous season. A 10 m × 10 m excavation square was set up (almost entirely within Braidwood's Operation J-II) using our benchmark (0,0) as a starting point, hitting a point 50–60

m to the northwest and 30–40 m to the northeast. It was cleaned and dug down (Fig. 2-1). We discovered various types of structures, such as a square-planned *pisé* building and well-preserved *tannor*, in Layers 5 and 6 (following Braidwood's Levels 5 and 6), and were able to capture a glimpse of Neolithic village life at Charmo.

Braidwood excavated approximately four meters below the surface for Operation J-II and up

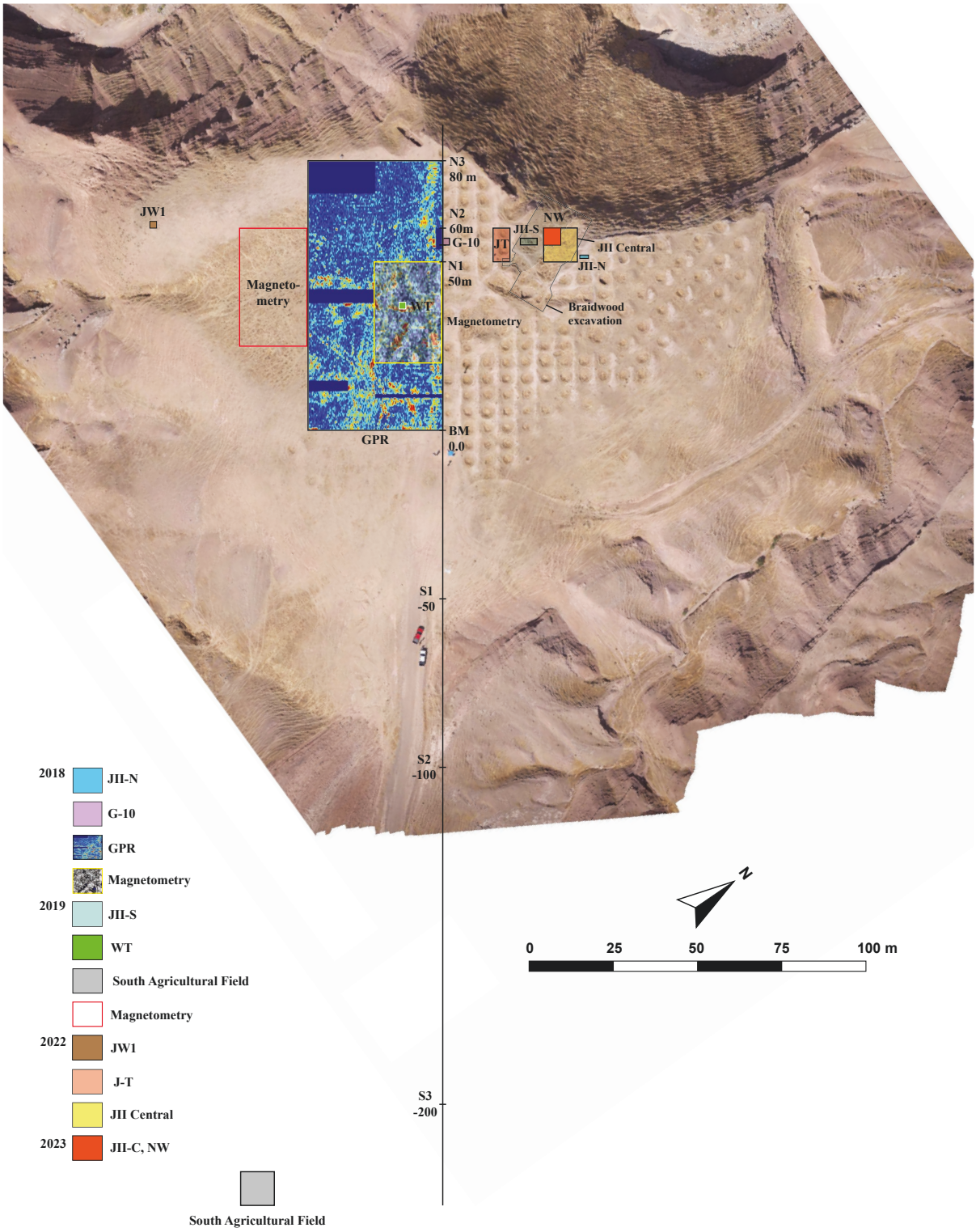

Fig. 2-1 Investigation squares in each season at Charmo.

to the sixth-floor level. Pottery was discovered from the top to Level 5, but no potsherds were discovered at Level 6. Therefore, the cultural deposits below Level 6 are Pre-Pottery Neolithic layers. We hoped to excavate the cultural layers below this Level 6 (we called it Layer 6) and to reach the virgin soil, because we learn more about the period when people began to inhabit the Charmo site.

Because this season's investigation was expected to last approximately 50 days, the digging area was limited to the northwestern portion of the J-II central square (5 m × 5 m) to reach the virgin soil (Fig. 2-2). We refer to this as the J-II central NW area. Therefore, an excavation square was set up, hitting a point of 55–60 m to the northwest and 30–35 m to the northeast from our benchmark (Figs. 2-1 and 2-2).

Layer 6, which was excavated in the previous season, was approximately 728 m asl. reaching the basement of the *pisé* building (Str. 10) and *tannor* (Str. 11). In this season's excavation area, J-II central NW, ash pits and ash deposits were found in Layer 7, just below Layer 6 (Figs. 2-3–2-5).

Animal bones, stone vessels, bone implements, and clay figurines were discovered in and around ash pits and deposits. One of the most beautiful artifacts was a complete bone spoon (Fig. 2-6). Its form is similar to the marble spoon excavated in the previous season, but it is thinner and more delicate, requiring high-quality craftsmanship.

When Layer 7, consisting of ash pits and ash deposits, was removed, a hearth (Str. 22) and stone cluster (Str. 23) began to be detected, forming cultural deposits, that is Layer 8 (Figs. 2-3 and 2-7).

The hearth (Str. 22) consisting of black ash deposits was found at the northeastern corner of the excavated square (Fig. 2-8). An animal clay figurine was discovered alongside the black ash (Fig. 2-9).

The stone cluster (Str. 23), consisting of flat sandstones, was discovered in the southern portion of the excavation area (Fig. 2-10). Possibly, it was a part of the stone foundation for a *pisé* wall or a lid stone for a pit structure, but no definite remains were detected in this structure.

In addition to these stone cluster and hearth structures, many building materials and mat fragments were discovered in this layer. Building materials consist of lumps of clay of various sizes containing a lot of chaff and sometimes with traces of mats. These were likely used as pisé, ceiling or flooring materials (Fig. 2-11).

More direct evidence was the presence of mat fragments (Fig. 2-12). These are woven reeds, such as baskets, and are the charred remnants of a ceiling or flooring material. Undoubtedly,

Fig. 2-2 UAV view of Charmo 2023 excavations.

these building materials were unearthed because houses and other buildings were located near the excavation area.

From the middle of Layer 8, the excavation area was further limited to 5 m × 3 m, hitting a point of 57–60 m to the northwest and 30–35 m to the northeast of our benchmark, and the excavation was continued. After the removal of Layer 8 structures, a 0.3–0.4m thick layer with no significant structures was detected (Layer 9 upper). Below that was a black ash layer more than 0.5 m thick. We named Layer 9 snail layer. This is because a very large number of snails, over 20000 in total, were excavated from this ash layer (Figs. 2-13–2-15).

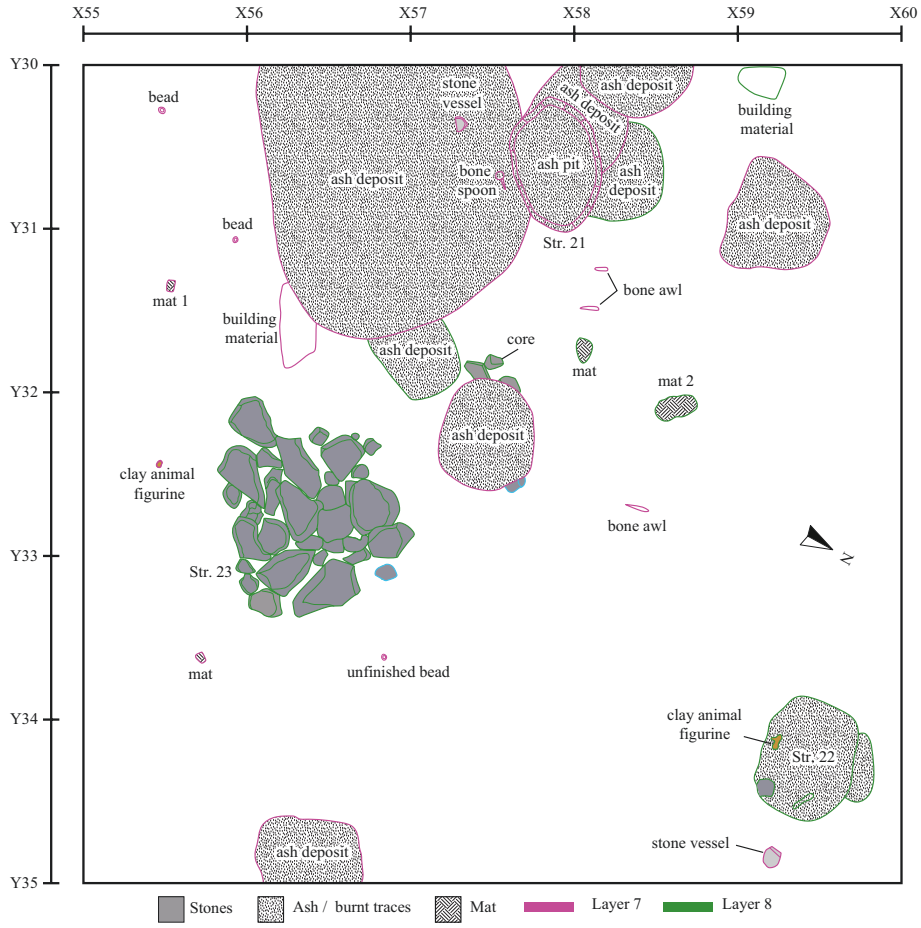

Fig. 2-3 J-II central, Layers 7 and 8 structures.

Fig. 2-4 Str. 21 (ash pit) in Layer 7.

Fig. 2-5 Ash deposits in Layer 7.

Fig. 2-6 Complete bone spoon discovered from Layer 7.

Fig. 2-7 General view of Layer 8 (from west).

Fig. 2-8 Hearth (Str. 22).

Fig. 2-9 Animal clay figurine discovered beside Str. 22.

Fig. 2-10 Sand stone cluster (Str. 23).

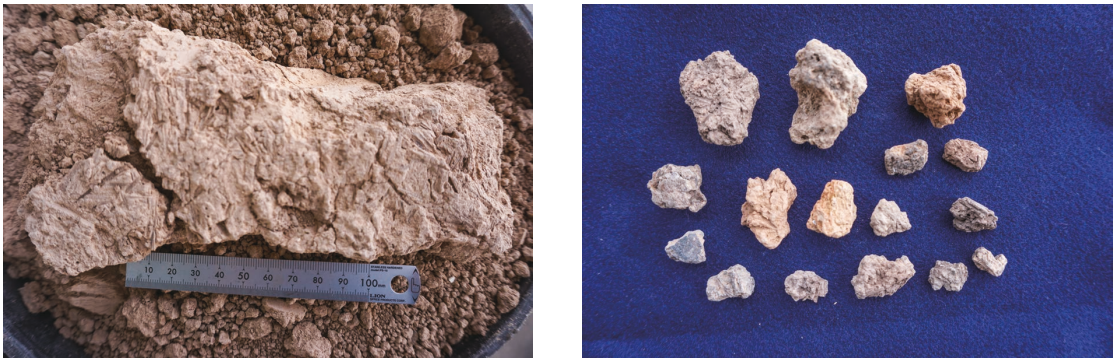

Fig. 2-11 Building materials discovered from Layer 8.

Fig. 2-12 Mat fragments discovered from Layer 8.

Fig. 2-13 Layer 9 snail layer.

Fig. 2-15 Large number of snails excavated.

Fig. 2-14 Digging the Layer 9 snail layer.

A small percentage of the snails were subjected to fire and turned blue. However, because many others appear to have been boiled, snails must have been used in their diet. The snails excavated were the same species, likely *Helix salomonica* Nägele 1899, a type of escargot. Therefore, it is assumed that the snails were edible to the Charmo people.

Layer 9 yielded not only a large number of snails, but also many clay figurines (Fig. 2-16), carbonized mat fragments (Fig. 2-17), carbonized seed deposits (Fig. 2-18), and animal bones (Fig. 2-19). These diverse and abundant objects indicate that this ash layer was a type of dumping ground within the Layer 9 settlement. The study of carbonized seeds and animal bones is expected to reveal specific food habits of the Pre-Pottery village at Charmo. We are particularly interested in the bones of large unearthed cattle. This is because, in the Pottery Neolithic and Pre-Pottery Neolithic layers at Charmo that we previously investigated, sheep and goat bones were overwhelmingly abundant,

whereas cattle and wild boars were rarely discovered.

Below the thick ash layer (Layer 9 snail layer) is a slightly harder cultural deposit of light yellow-orange color, with scattered limestone and sandstone and many animal bones. We named it Layer 10 (Fig. 2-20).

As in Layer 9, carbonized seed deposits (Fig. 2-21) and clay figurines were discovered in this layer. Interestingly, flat circular clay balls were found in these clusters (Fig. 2-22). Notably, four well-polished stone axes were found in close proximity to each other, indicating deposits of some type (Fig. 2-23).

Fig. 2-16 Large animal clay figurine.

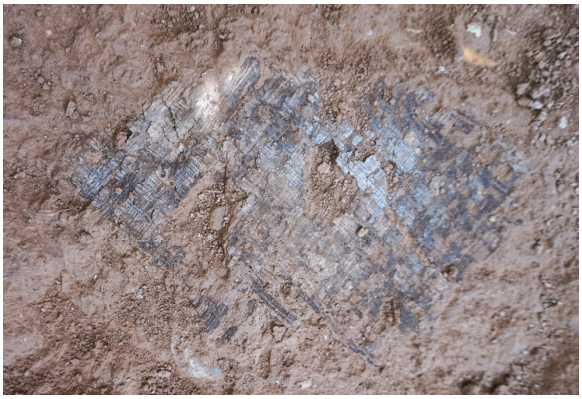

Fig. 2-17 Carbonized mat fragment.

Fig. 2-18 Carbonized seed deposit.

Fig. 2-19 Astragalus of a huge cattle.

Fig. 2-20 General view of Layer 10 from east.

Fig. 2-21 Carbonized seed deposit.

Fig. 2-22 Flat and circular clay objects found in Layer 10.

Fig. 2-23 Well-polished stone axes discovered in Layer 10.

Further excavation revealed a *pisé* wall and mud-plaster floor east of the excavation area (Figs. 2-24–2-25). It was assumed to be part of a rectangular plan building (Str. 24). Therefore, we identified the cultural deposits in which this building was located as Layer 11. The remaining *pisé* wall in the northern section of the excavation area accounts for at least four stages (Fig. 2-26). An adult burial (Sk5) was found in a pit dug into this *pisé* building (Fig. 2-27). Based on these findings, it was possibly an underfloor burial of the rectangular *pisé* building.

After removing the buildings and artifacts discovered in Layer 11, we reached a reddish-brown colored marginal virgin soil at an elevation of approximately 725 m asl (Fig. 2-28).

Rough dwelling-pit-like structures (Strs. 26 and 28) dug down into the virgin soil of marl. A small ash pit (Str. 27) was also discovered in virgin marl soil (Figs. 2-29 and 2-30). It can be assumed that these dwelling-pit-like structures were detected from the lowest cultural deposits at Charmo. Therefore, these structures can be considered the earliest evidence of living at Charmo.

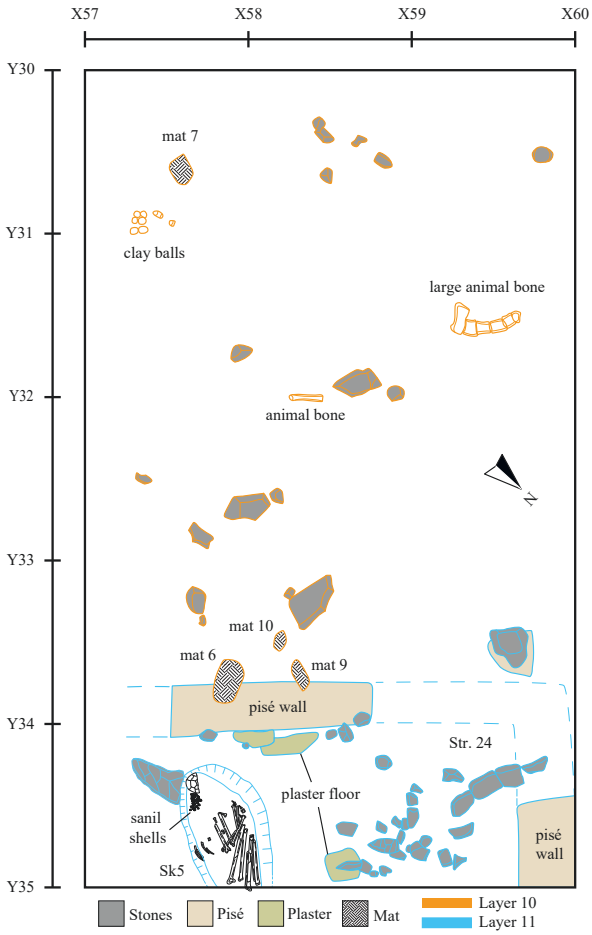

Fig. 2-24 J-II central NW, Layer 11 structures.

Fig. 2-25 *Pisé* building in Layer 11.

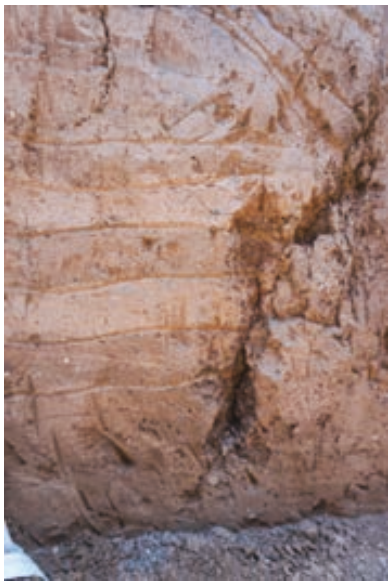

Fig. 2-26 Remains of the *pisé* wall in the section of the excavation area.

Fig. 2-27 Adult burial discovered within the *pisé* building.

Fig. 2-28 Layer of marl that appears to be the virgin soil beneath Layer 11.

Interestingly, a goat mandible was discovered with a small flint point just above the western wall of Str. 28 (Fig. 2-31). Using imagination, this may be interpreted as the beginning of Charmo village, when the people began to build simple dwelling pits for hunting, herding or other activities on the Charmo marl. Topographically, Charmo is higher than the surrounding hills, even at 725 m asl, with the elevation of the virgin soil ground immediately below Layer 11. In any case, it can be assumed that the first people to come to Charmo set up a camp here, probably because it had a good vantagepoint that was suitable for hunting or other activities.

In addition to the ash pit and goat mandible, a clay figurine that might have been a wild boar (Fig. 2-32), carbonized seeds (Fig. 2-33), and the entire rodent skeleton (Fig. 2-34) were excavated above the virgin soil, suggesting that a variety of activities took place on the virgin soil.

In the J-II central NW area, we reached the virgin soil at approximately 725 m asl, which is approximately three meters deeper than Layer 6 excavated by Braidwood (Fig. 2-35). We collected approximately 70 carbon samples for ^{14}C dating from the excavated area to determine the absolute age of Charmo's earliest village.

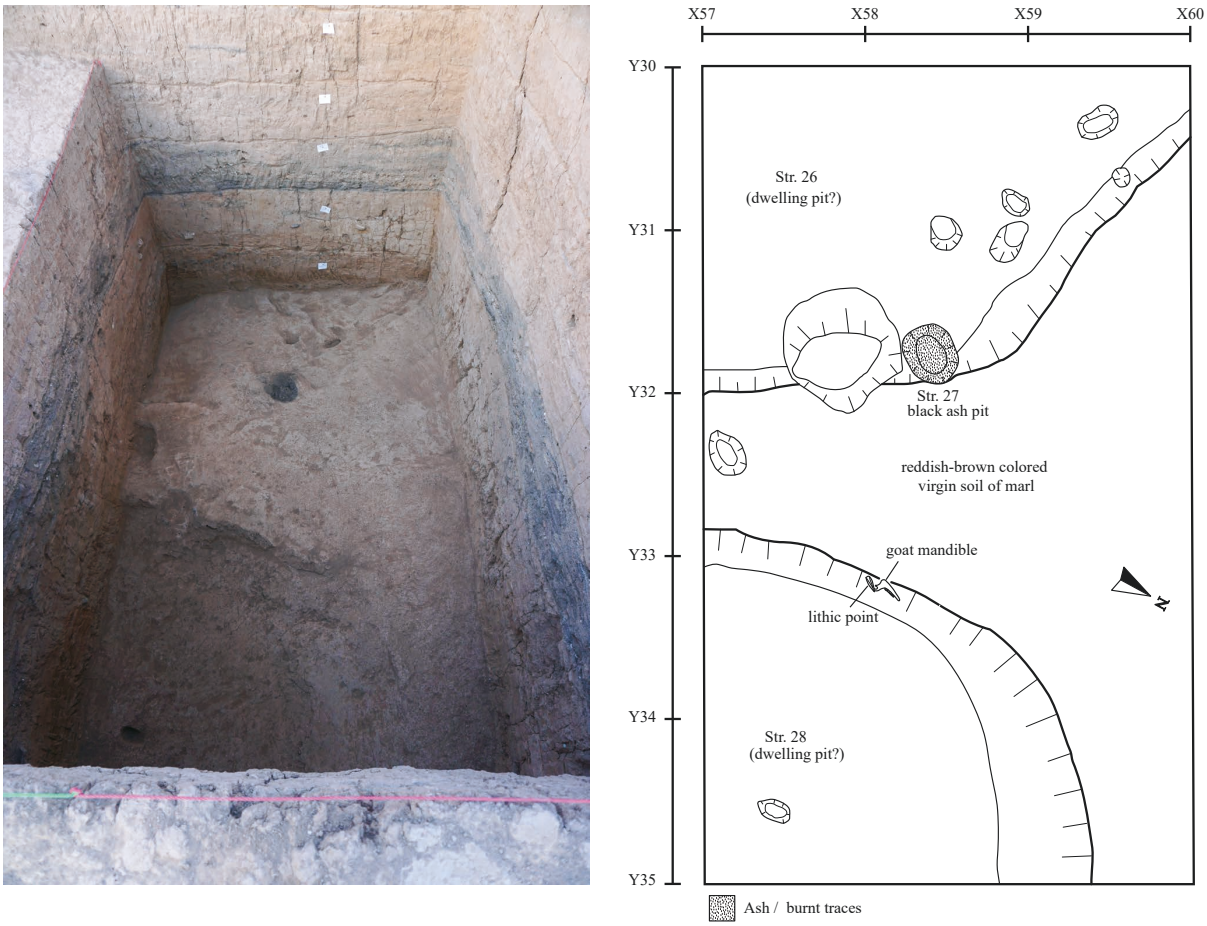

Fig. 2-29 Dwelling pit-like structures discovered beneath of Layer 11 on the virgin-soil.

Fig. 2-30 Small ash pit found at the periphery of Str. 26 dwelling pit.

Fig. 2-31 Goat mandible discovered with a small flint point at the periphery of Str. 28 dwelling pit.

Fig. 2-32 Clay figurine of the wild boar.

Fig. 2-33 Carbonized seeds.

Fig. 2-34 Rodent skeleton.

Fig. 2-35 North section of the J-II central NW area.

(Akira Tsuneki)

3. Neolithic burials at Charmo, the 2023 season

Excavations in the 2023 season were concentrated in J-II central NW area. The skeletal remains of six individuals were identified during the two excavation seasons (2022 and 2023) (Table 3-1). During this season, the remains of two human skeletons were excavated, one from Layer 8 and the other from Layer 11, both belonging to the Pre-Pottery Neolithic (PPN) cultural layers (Table 3-1).

Table 3-1 Skeletal remains from Charmo.

	Skeleton No.	Square	Year	Layer	Age	Sex	Burial type	Position	Body axis direction	Face direction	Grave goods	Grave pit
1	Sk1	JT	2022	5	5yrs - adolescent	–	unknown	–	–	–	–	–
2	Sk2	J-IIC	2022	5	Adult	–	unknown	–	–	–	–	–
3	Sk3	J-IIC	2022	6	2–5yrs.	–	unknown	–	–	–	–	–
4	Sk4	J-IIC NW	2023	8	adult 40–60yrs.	–	unknown	–	–	–	–	–
5	Sk5	J-IIC NW	2023	11	adult 40–50yrs.	male	Primary	Left	Flexed position	N	–	Shallow grave pit
6	SK6	JT	2022	5	adult	–	unknown	–	–	–	–	–

Sk4

It is a fragment of a human adult cranium discovered at the bottom of Layer 8 near the northwestern wall of the J-II central NW (Fig. 3-1). The cranium was buried below the corner of the whitish-yellow floor. As the rest of the floor is outside the excavation area, it is not clear whether the location of the cranium is associated with the floor. The other half of the cranium and other skeleton parts were missing. It was difficult to determine the burial type; therefore, it was classified as unknown. No evidence of a grave pit or grave preparation was found.

Sk5

Sk5 is the primary burial of an adult, probably a male, discovered at the eastern edge of Square J-II central NW in Layer 11 (Fig. 3-2). Parts of the skeletons were outside the excavation area. The preservation condition of the bones was relatively good, except for the skull. The deceased was buried in a tightly flexed position on the left side. The body axis direction was west-east, and the head pointed to the west. Based on the deposition of the skull, it likely faced north.

The skull and upper body were initially located beneath the steps made to exit the excavation square. Workers smashed the frontal part of the skull while cleaning the step section; therefore, the

Fig. 3-1 Sk4 A fragment of an adult cranium.

Fig. 3-2 Sk5.

mandible and maxilla were damaged. The rest of the skull remains intact in the step section. After removing these steps, the skeleton was revealed; however, some skeletal parts were missing. The upper body was twisted, and it is not clear whether the skeletal remains were under the wall section. The skull, maxilla, mandible, a few ribs and vertebrae, and upper and lower limbs are present. The head was leaned beside a large sandstone located behind the skull. Notably, approximately 25 snail shells were found at neck level at the base of the skull. Snail shells are likely to have been intentionally brought to this place in relation to a funerary rite.

Initially, the bones of the lower and upper limbs were discovered; however, not all bones of the hands and feet were present *in situ*. The legs were tightly bent as if they were tightened by a rope, both arms were bent, and the hands were placed over the knees. The hipbone was not extracted because it was out of the excavation area in the eastern section.

Regarding the spatial location of the burial, the deceased was buried in a shallow grave pit beneath a mud-plastered floor (Fig. 3-3). In addition to the grave pit, there was a *pisé* wall on the west side and a short row of small stones on the north and east sides. Another small *pisé* wall was discovered to the north of the stone. These structures are probably related to the rectangular plan building (Str. 24) in Layer 11 (Fig. 3-4). The burial was likely associated with the building, and the grave pit was dug through the floor of the room.

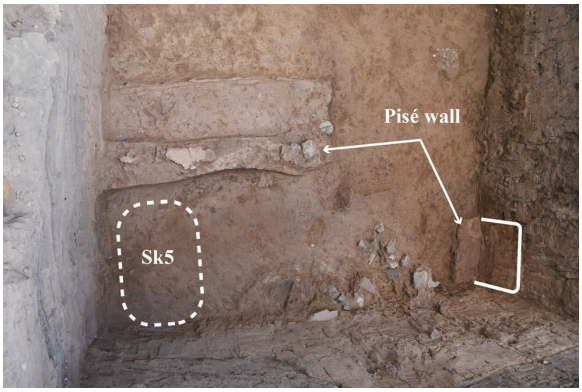

Fig. 3-3 Location of Sk5.

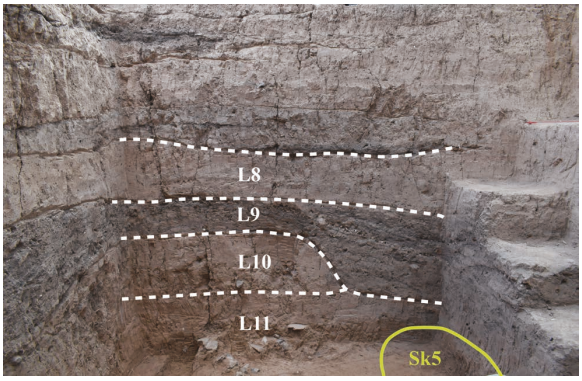

Fig. 3-4 Eastern wall section of Square J-II central NW area.

Sk6

Sk6 is a fragment of a human skull excavated during the 2022 excavation season in Layer 5 in the NE part of the J-II central square, as reported by [Tsuneki *et. al* 2023: 28] (Fig. 3-5). No number was provided at that time to conduct further analyses. Analyses of the skeletal elements by Y. Miyauchi indicated that the fragments belonged to an adult individual.

Fig. 3-5 Sk6 bone fragment.

Conclusion

Remains of six individuals were discovered at Charmo during the 2022 and 2023 excavation seasons. Five of the six individuals were partially represented by different skeletal elements. One of the individuals was primarily buried beneath the floor of a building, but lacked some skeletal elements. The other five individuals were buried in different contexts, such as next to a *tannor*-like structure, in a charred layer, or beside a structure building. However, the relationship between human remains and these structures is not clear. In general, human remains discovered in Charmo have not provided information that helps us understand and estimate the Neolithic burial customs in the eastern part of Zagros.

A noteworthy discovery was the large number of snail shells in the thick layer (Layer 9) and at the neck of Sk5 in Layer 11. Snails are mollusks used in different cultures worldwide as a source of food and in rites. Both intact and cremated snail shells were uncovered at Charmo. The large number of snail shells uncovered in Layer 9 indicates that they were consumed by people in different ways and that the nearby Cham Gawra River was the source of the snails.

The presence of snail shells in large quantities may be associated with ritual feasts or a symbolic significance event, and the snails were prepared and consumed during these events. On the other hand, the snail at the neck of Sk5 might have been dedicated to the dead as a ritual practice or grave goods.

(Sari Jammo)

4. The human remains from Charmo (2022 and 2023)

Aim and scope of the analyses

This is a preliminary report on human remains found at Charmo (Jarmo) during an archaeological mission from the University of Tsukuba in 2022 and 2023. Charmo is located in northern Iraq in the Chamchamal area, on one of the hills along Cham Gawra. The site was excavated between 1948 and 1955 by the Jarmo Prehistoric Project, led by Professor Robert J. Braidwood of the University of Chicago, to study the Neolithization process in the region. The cultural deposits date from the Pre-Pottery Neolithic to the Pottery Neolithic periods. In addition to a detailed description of the human remains found in 2022 and 2023, this report also provides an overview of the human remains found during the 1940s and 50s, as well as previous analyses. It should be noted that the unexcavated areas of the site may contain additional human remains.

Human remains recovered from the excavations during the 1940s and 50s

Several burials were found during excavations between 1948 and 1955 [Braidwood *et al.* 1960, 1983]. Human remains designated by identification codes S1 to S6 were reported from the J-I operation, S1 to S5 from the J-II operation, and one burial near the M20 square [Braidwood *et al.* 1983: 427]. The results are summarized in Table 4-1. Charlotte M. Otten (University of Chicago) and Fredrick Barth (Ethnographic Museum of the University of Oslo) performed field observations, but no detailed information on human remains has been published yet. Burials were generally articulated. However, the burials lacked uniformity in skeleton positioning. There were no traces of grave pits, except for one case (J2-S3), and no grave goods. Given the limited number of recovered burials and seeming attention afforded to the burials, it was suggested that the Charmo people buried their dead at an off-site cemetery [Braidwood *et al.* 1983: 427]. All human remains recovered during the 1940s and the 1950s belong to the Pottery Neolithic period (Table 4-1).

Detailed studies on the cranium from J2-S4 were conducted by Sherwood L. Washburn from the University of Chicago and J. Lawrence Angel from the University of Pennsylvania, Baugh Institute of Anatomy. The prevailing research interest at the time was the origin of the populations, based mainly on the facial morphology of the cranium. Washburn reported that the cranium was "completely modern" with a "very high-ridged nose" [Braidwood *et al.* 1983: 427], whereas Angel observed that "the general impression is a face showing Iranian and well as Mediterranean traits" [Dahlberg 1960: 248].

Albert A. Dahlberg from the Zoller Laboratory of Dental Anthropology at the University of Chicago analyzed 96 permanent and 30 deciduous teeth from seven individuals to explore genetic and nongenetic dental features [Dahlberg 1960]. Dahlberg concluded that the dental features from Charmo were similar to those of modern Mediterranean and European populations and that the

Table 4-1 Summary of the human remains excavated by Braidwood [Braidwood *et al.* 1983].

Square	Year	Skeleton number	Age	Sex	Bone preservation	Location/ Layer	Position of body	Grave pit	Grave goods	Remarks
J-I	1948	S1	infant	cba	articulated	Uppermost meter of deposit	Flexed, facing opposite directions	No	No	Recent burial?
		S2	infant	cba	articulated					
		S3	adult	indet	articulated	Third floor in the corner of a portion of pisé walling	Supine, flexed, facing South?*	No	No	Accidental death by roof cave-in?
		S4	adult	indet	articulated		Flexed?*			
		S5	adult	indet	articulated		Supine? flexed*			
		S6	adult	indet	articulated		Left side down, flexed*			
J-II	1950	S1	–	–	articulated	Clearance of the first floor	–	No	No	Recent burial?
		S2	youthful/ young adult	indet	disarticulated	Second floor	–	No	No	
		S3		indet	disarticulated	Second floor, partly overlying S4	–	No	No	
		S4	adult	male	articulated		Prone, facing West	Yes	No	
		S5	early teens	female	articulated	Cleaning of the second floor	Supine, flexed	No	No	Accidental death?
Near M20	1955	–	adult	indet	articulated	0.75 m in depth	–	No	No	

cba: cannot be assessed
indet.: indeterminate
* inferred from Braidwood *et al.* 1983, Fig 172

dental attrition pattern indicated the absence of gross, coarse particles in their diet. However, the specific individuals included in Dahlberg's analyses were not clearly stated in the publication.

Human remains excavated during the 2022 and 2023 season

Materials

Six individuals were recovered in 2022 and 2023 from Charmo in the J-II central square and JT square (Table 4-2). In 2022, three individuals, represented mainly by cranial remains and consisting of both non-adults and adults, were found in the J-II central square. One individual was recovered from the JT square. In 2023, the first primary burial discovered during the two previous excavation seasons was found in the northeast part of the J-II central square. Furthermore, a fragment of an adult cranium was found in the northwestern part of J-II central square. The following subsections outline the results of macroscopic and metric analyses of these remains.

Methods

Sk (abbreviation of "skeleton") number was allocated to the accumulation of human bones. It is noteworthy that a single Sk does not necessarily represent a single individual.

The age-at-death of adults was estimated comprehensively based on suture closure of the cranium [Meindl and Lovejoy 1985] and dental attrition [Lovejoy 1985] in the absence of other viable indicators (*i.e.*, auricular surface of *os coxae,* pubic symphysis). Due to the highly fragmented state of preservation and the limited elements recovered, the age-at-death of non-adult individuals (under 16 years old) was estimated by size comparison with reference models (©Bone Clones, Inc.: fetus SCM-186-D, 14–16 months old SC-187-DH, 5 years old SC-183-DH, and 13 years old FM-509-SET) to narrow the age range. These reference models were cast from the original bones of modern specimens. Based on a size comparison with the reference models, the age range was divided into a full-term fetus, fetus-2 years, 2 years, 2–5 years, 5 years, 5–13 years, and indeterminate non-adult. However, it should be noted that age estimation based on size comparison is only approximate and is less accurate than other methods (*i.e.*, dental development, fusion of epiphyses, and bone measurements).

Sex estimation was based on the cranial morphological characteristics outlined by Walker in Buikstra and Ubelaker [1994] and the morphological characteristics of the postcranial bones. Sex cannot be morphologically estimated based on non-adult bone elements that have not yet developed secondary sexual characteristics. The stature of adults was estimated using the American white male and female formulae from Trotter [1970] and formulae for all population groups from Sjøvold [1990], as no population-specific methods exist for the relevant population.

When Sk was represented only by the cranium, the preservation ratio of the cranium was indicated by percentages of $<25\%$, 25–50%, 50–75%, and 75–100%.

Table 4-2 Overview of the human remains from Charmo (seasons 2022 and 2023).

Sk no.	Square	Layer	Age	Sex	Stature
Sk 1	JT	5	5–13 years old	cba	
Sk 2	J-II central	5	adult?	indet	
Sk 3	J-II central	6	2–5 years old	cba	
Sk 4	J-II central	8	40–60 years old	indet	
Sk 5	J-II central	11	40–50 years old	probable male	176.91 ± 4.32 cm [Trotter 1970] 174.99 ± 4.97 cm [Sjøvold 1990]
Sk 6	JT	5	adult	indet	

cba: cannot be assessed
indet.: indeterminate

Results

Human remains excavated during the 2022 season

Contextual information on burials from 2022 is available in Tsuneki *et al.* [2023: 27–29].

Sk1

Sk1 is represented by small indeterminate calvarium fragments. These fragments were found at a depth of approximately 3 m in Layer 5 of the JT square. The size of the calvarium fragments indicates an age of approximately between 5 and 13 years. Preservation of the cranium was <25%.

Sk2

Sk2 is represented by the frontal bone. This frontal bone was found in Layer 5 on the western wall of the J-II central square. The right orbit of the glabella was preserved with fragments of the frontal squama. The size of the bone is close to that of an adult but relatively gracile. The score of the glabella for sex estimation was 1. However, sex estimation based on only one feature may be problematic; therefore, sex was not estimated. Preservation of the cranium was <25%.

Sk3

Sk3 is represented by indeterminate small fragments of the calvarium of a non-adult, probably between 2–5 years old, based on the thickness of the bone fragments. It was found on the floor of a pit in the J-II central square, north of a structure building (Str. 10). The association between human remains and buildings is discussed. Preservation of the cranium was <25%.

Sk6

Sk6 is a newly identified individual from bone fragments found in the northeast part of the JT square in Layer 5. A new Sk number was given in 2023, as no Sk number was allocated to the bone fragments collected from this area during excavation. It is represented by the left orbital part of the frontal bone and the left greater wing of the sphenoid. The size of the frontal bone was similar to that of an adult; however, the frontal suture was persistent. Sex estimation is not possible because of the lack of sex diagnostics within the recovered elements. Preservation of the cranium was <25%.

Human remains excavated during the 2023 season

Sk4

Sk4 is part of an adult cranium. It was found at the bottom of Layer 8 near the northwestern wall of the J-II central square. 2/3 of the posterior right parietal, 1/4 of the posterior left parietal, and 1/3 of the superior occipital region were preserved. The sagittal suture was completely fused and the line was mostly obliterated. Sagittal and lambdoidal sutures around the lambda are slightly visible on the endocranial surface but are completely obliterated on the ectocranial surface. The age of an individual is estimated to be approximately 40–60 years old. No sex diagnostics were available. Preservation of the cranium was 25–50%.

Sk5

Sk5 was the first primary burial found during the two previous excavation seasons from the eastern edge of the J-II central square in Layer 11. However, the cranium is poorly preserved. Fragments of the parietal and distal parts of the right supraorbital margin, right and left temporal, right and left zygomatic, right part of the maxilla, and mandible were preserved. Postcranial elements included the proximal part of the clavicle, right and left humeri, radii, ulnae, carpals, metacarpals, hand phalanges, patellae, femora, tibiae, and fibula. Vertebrae and rib fragments are very few, which may be due to the disturbance from the upper layer [Prof. Tsuneki, personal communication]. The pelvic area and foot bones were not recovered, but there is a possibility that they remained in the excavation trench section. The excavation and analysis of such unexcavated elements, still within the archaeological strata, can only be completed during future excavation seasons.

Sex: Sexual dimorphic features of the cranium from the left mastoid process and right supraorbital

margin are indeterminate. However, the postcranial bones are robust, which gives the impression that the individual was probably male.

Age: The age was estimated to be 40–50 years old from dental attrition.

Stature: The stature was estimated from the length of the left ulna (278 mm). Using the formulae for American white males from Trotter [1970], the stature was estimated to be $3.70 * 27.8 + 74.05 = 176.91 \pm 4.32$ cm. Stature estimation using the formulae for all population groups from Sjøvold [1990] is $4.61 * 27.8 + 46.83 = 174.99 \pm 4.97$ cm.

Pathologies: Ante-mortem tooth loss was observed on the left side of the mandible. The alveoli from the first to third molars were completely closed and resorbed (Figs. 4-1A, B). The height of the resorbed part of the mandibular body was 18 mm. Linear enamel hypoplasia was observed in the upper canines (Fig. 4-2).

Other features: All roots of the teeth and some bones were discolored green (Fig. 4-3). According to pXRF measurements by Professor Ryo Anma from Tokushima University, the discolored area contained significantly more manganese than the other areas measured [Prof. Anma, personal communication]. This discoloration was likely due to the post-mortem uptake of manganese from the soil.

Other human remains with no Sk number

The following outlines the results of the macroscopic observation of the bone fragments found in 2022 with no allocated Sk number.

Within the label "Human Bones?" are fragments of the calvarium and indeterminate bone

Fig. 4-1A Mandible of Sk5, superior.

Fig. 4-1B Mandible of Sk5, lateral.

Fig. 4-2 Upper canines of Sk5 with linear enamel hypoplasia (white arrows).

Fig. 4-3 Discolored tooth from Sk5.

fragments.

Within the label "Square J-II Central SW Basket no. 44, Underneath the floor of Str. 10" are fragments of the calvarium of indeterminate age.

Discussion and conclusions of the human remains from 2022 and 2023

Remains of a total of six mostly incomplete individuals were recovered during the 2022 and 2023 seasons at Charmo. They were found in layers from the end of the Pre-Pottery Neolithic to the beginning of the Pottery Neolithic. The remains were highly fragmented, except for Sk5, which was an articulated burial. Both adults and non-adults were found in both squares. One non-adult and one adult were found in the JT square. From J–II square, two adults, one probable adult, and one non-adult were found. Sex estimation was not possible for most individuals because of high fragmentation and lack of sex diagnostics within the recovered elements. Sk5, found in 2023, was the first primary burial discovered during the two past excavation seasons. Sk5 is a probable male, approximately 40–50 years old. The teeth and mandible show signs of strong physical stress and ante-mortem tooth loss, pointing to further research directions regarding health and disease during the transition from the Pre-Pottery Neolithic to the Pottery Neolithic period.

(Yuko Miyauchi and Kirsi O. Lorentz)

5. Figurines and other clay objects from Charmo

Excavations during the 2023 season were concentrated in the J-II central square in the northwestern part. Various types of objects made of different materials were discovered, including clay figurines and other clay objects. All clay objects described in this report were discovered between Layers 6 and 11, and a few from the surface layers. Clay objects were among the most remarkable discoveries made during the excavation season. Some objects were illustrated on an actual scale. Also, sophisticated figurines were documented using three-dimensional (3D) modeling. In addition, five broken or need-to-be-clean figurines were transported to Japan for cleaning, restoration, and analysis, and they will be returned to the Slemani Museum.

Study process

According to Braidwood's final report in 1983, more than 5,000 figures and other clay objects were discovered [Morales 1983]. By the end of the 2023 excavation season, 83 clay objects were uncovered. Clay objects are artifacts made of clay, unbaked or originally made of clay, and exposed to fire at certain levels. Clay objects include human figurines, animal figurines, small and large clay balls and other geometric forms. Some of the shapes of the clay figurines/objects were identified; however, others are unclear, and further analyses are required.

The color of the clay of the figurines/objects tended to be darker than the surrounding soil in which they were discovered. Generally, their color was brown and dark brown; therefore, they were in many instances easily identified during excavation; however, after drying, the color of some clay objects turned greyish brown. It is not clear whether a particular type of clay was used to manufacture the figurines/objects or if the clay was mixed with other materials. Scientific analyses were conducted on a number of samples to determine the clay content. Among the clay objects, at least two pieces were coated with a visible red color, probably ochre.

The production technique of the figurines and other objects was relatively good. The surfaces of a few clay figures were smooth; however, others were coarse with cracks. None of the figurines were baked; however, a few seemed to have been partially exposed to fire, and black-carbonized traces were visible on the surface. Despite the discovery of several fireplaces, there was no evidence of baking the figurines, indicating that some figurines might have been accidentally exposed to fire.

Although not all clay figurines/objects were sufficiently dry, light cleaning was carried out using soft brushes and dental tools.

Figurines and other clay objects

Clay figurines/objects were discovered in all the excavated layers, including the surface layer. The largest number of clay figurines/objects were discovered in Layer 9, or the so-called *snail layer* (a large number of snail shells were discovered), Layer 8, and Layer 10 (Fig. 5-1). A few clay figurines/objects were discovered intact; however, the majority were fragmented or had missing parts, which made it difficult to determine their shape. The sizes of the clay figurines/objects were relatively small ranging from 2 to 10 cm. The largest figurine represents an animal (No. 39). The back half of the figurine (legs, tail, and parts of the body) is preserved; however, the head part is missing.

Clay figurines/objects were sorted into seven groups (Fig. 5-2): animal figurines, human figurines, geometrically shaped clay objects, fragments of figurines, sherds of clay vessels, ovoid-shaped clay objects, and unclassified clay objects. The final classification can be modified based on further discoveries and studies.

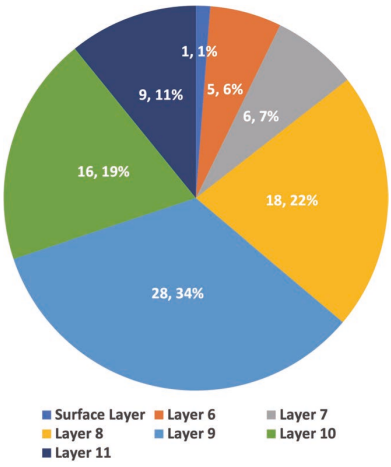

Fig. 5-1 Distribution of clay figurines / objects.

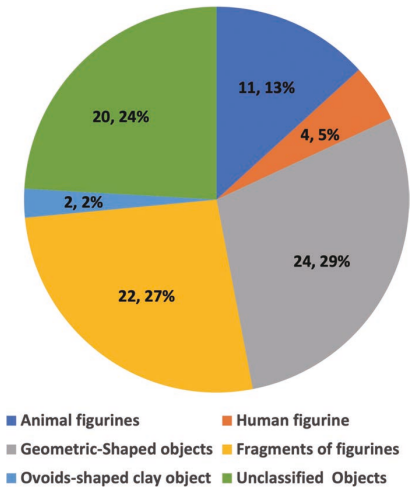

Fig. 5-2 Clay objects typology.

Animal figurines

Animal figurines were well elaborated, representing a sophisticated artistic sense. A minimum of 11 animal figurines were discovered (Fig. 5-3). The animal shapes of some figurines were clearly observed; however, it was difficult to identify the exactly represented creatures in some instances. The face or facial elements for the five examples were missing or broken; hence, they were difficult to categorize. All figurines were missing tails, except for two (No. 39 and 68) with short extensions. Based on the animal figurine shape, three categories were identified: wild boars, dogs, and horned animals (sheep or goats). In addition, some animals were represented partly by the partition of the body and parts of the limbs, called indeterminate figurines. Animal figurines were standing on their limbs, sitting with the limbs extended, or sitting straight on their legs. The forelegs and legs of two figurines (nos. 38 and 56) were combined, with the base resting on.

The best-preserved animal figures are No.16, 40, and 68. No. 16 and 40 represent dogs and No. 68 represents a wild boar. The latest is small but the most beautiful among the animal figurines collected during this season. The wild boar is approximately 3 cm long standing on its limbs. It has a short, rounded nose, the left eye is visible, and the left ear is at the top of the head (the right

eye and ear are broken off). The head is connected to the body; therefore, there is no neck. It has an accentuated spine at the center of the back extending straight to the tail, which is missing.

Fig. 5-3 Animal figurines.

Human figurines

The number of human figurines uncovered from Charmo during this season was limited (4 figurines). Unlike animal figurines, no complete human figurine was discovered (Fig. 5-4). The figures are small (less than 5 cm). The figurines were incarnated and were likely depicted as females. These human figurines from Jarmo are similar to some extent to female figurines discovered during Braidwood's excavations, and to those from neighboring regions [Morales 1983; Zeidi and Riehl 2012].

Fig. 5-4 Human figurines.

Two of the figurines (No. 15 and 42) are in a standing position on a conical base and have their head broken off. One (No.15) was made with a band-like shape wrapped around the waist, forming a visible protrusion resembling a node at the joint point. The other one (No. 42) has a protrusion in the chest area on one side of the body (probably depicting breasts). Another one (No. 30) is simply made and consists of fragments that seem to have been composited together. The head and body parts exist, and the bottom part is broken. The head is bent down with a notch, dividing it into two halves; however, no facial features were observed. The last one (No. 53) is represented by a portion of a clay figurine, probably in the sitting position. A pair of legs and part of the bottom of the body are present, but the top is broken, and no head was preserved.

Geometric-shaped clay objects

Geometric clay object collection was a remarkable discovery at Jarmo, and they were modeled in shapes that included balls, discs, cylinders, and polyhedrons (Fig. 5-5). In general, these objects were devoid of markings, had plain and smooth surfaces, and some appeared to be incomplete. The most common objects were balls and discs of different shapes, sizes, colors, and finishes. One small clay ball (No. 59) was special, depicting a head with eyes and nose, indicated by small holes. Some of the balls were not finished or well-modeled, with irregular grooves on the surface, and were discarded.

Fig. 5-5 Samples of geometric-shaped clay objects: no. 46-1, no. 75 differently finished clay balls; no. 76 smashed or discarded clay ball; no. 37 clay disc; no. 36-2 Polyhedron-shape; no. 59 head.

In Layer 10 of the excavation square, unique assemblages of clay balls were excavated next to each other in the same place (Fig. 5-6 middle). The assemblage comprises two types of balls, and at least seven clay balls were discovered. The first type comprises four balls arranged in a circular form around the fifth ball in the center (Fig. 5-6 right). The balls were solid and intact; however, some broke off during the excavation. The second type comprises two clay balls (Fig. 5-6 left). The upper parts of the balls broke off during the excavation; however, they were spherical hollow clay balls. No specific elements were found on the balls. The balls were wet, fragile, and left to dry before restoration and surface cleaning. These hollow balls are among the oldest of their kind in the Near East. The purpose of these artifacts is not yet clear; -although it is early to assume- they seem to be like hollow clay balls or sphere-shape that contain geometrical shapes "tokens" connected to the beginnings of literacy in the succeeding periods in the ancient Near East.

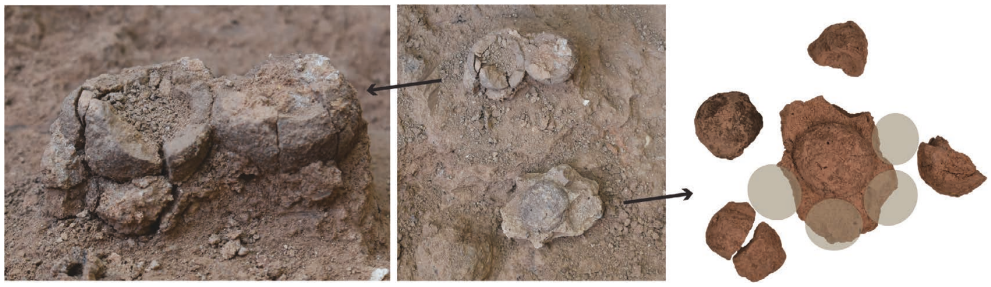

Fig. 5-6 Assemblages of clay balls. Left: hollow clay balls; right: assembly of five clay balls.

Fragments of figurines

This collection contains 22 objects found in different parts of the excavation area (Fig. 5-7). These are fragments of a variety of parts of clay figurines that probably broke off of their original bodies. This collection contains conical and circular bases of figurines (10 samples), cylindrical parts of figurines (seven samples), stalk figurines (three samples), and upper parts of figurines (two samples).

Fig. 5-7 Fragments of figurines: no. 6 of clay figure depicted with red ocher; no. 11 and no. 60 figurines with conical bases; no. 29 parts of figurine body; no. 34 and no. 43 stalk-type figurines.

One of the remarkable samples in this collection is a fragment of a clay figurine coated with a red pigment. This object was brought to Japan for restoration and analysis. Preliminary analysis indicated that the pigment was red ochre.

Ovoid-shaped clay objects

A distinctive discovery among the collections of clay objects was the presence of two ovoid-shaped samples. Their shapes are unique, and the purpose of using these types of objects remains unclear. The first sample (No. 55) was not intact; only half of the object was uncovered, whereas the other half was missing. Its color was dark, probably owing to deep firing. The second sample (No. 77) (Fig. 5-8)

Fig. 5-8 Ovoids-shaped clay objects.

was also fired, and a dark black color was visible on the surface. The sample was intact, but fragile when excavated; however, some parts broke up during moving.

Fig. 5-9 Unclasified clay objects.

Unclassified clay objects

Unclassified clay objects refer to a collection of 17 objects discovered in the same contexts as other clay objects (Fig. 5-9). They are neither complete nor have a particular shape. Therefore, they are difficult to classify. They are likely parts of clay figurines/objects, discarded objects, or residues when clay objects were manufactured. One object (No. 12) was unique with a hollow pointed end and two small holes on either side of the pointed end.

(Sari Jammo)

6. Other objects discovered during the 2023 excavations

Excavations in the Charmo J-II central NW area in 2023 investigated layers below Layer 6, which was excavated in the previous season. A wide variety of objects were discovered from each layer, from Layer 6 to the pit-dwelling structures dug down from Layer 11's virgin soil. Here, we present a summary of the artifacts, excluding natural remains such as human bones, animal bones, and carbonized plants. Note that the clay objects were reported in the previous section.

Stone and clay vessels

A few potsherds were recovered from Layer 5 last year, but none were discovered in Layer 6. During this season's investigation, not a single potsherd was recovered from the Layers 6–11 cultural deposits, except for a few pieces recovered during the cleaning of the fill in the previous season's research area on the first day of the season. In other words, all the cultural strata investigated this season were from the Pre-Pottery Neolithic period; thus, stone vessels replaced pottery as container vessels. Fifty-seven stone vessels of various sizes made of marble, limestone, and sandstone were excavated. Most were small fragments; however, some contained whole forms that could be reconstructed. The marble vessels were often bowl-shaped with a curved body and semicircular cross section, ranging from small (Fig. 6-1:1) to medium sized (Fig. 6-1:2). Some vessels had a body that was not curved but rather extended in a straight line toward the rim (Fig. 6-1:3). The marble vessels were beautifully polished. The limestone vessels were mainly medium-to-large-sized, but most were fragments and could not be reconstructed into their original shape. The sandstone vessels ranged in size from small to large (>30 cm in diameter). Shallow bowls (Fig. 6-1:4) were prominent, but there were also semicircular bowls (Fig. 6-1:5) and large bowls (Fig. 6-1:6).

Stone vessels were discovered in the lowest layers, 11 to 6, and there is no doubt that some were from the Charmo Pre-Pottery Neolithic village. They were recovered from Layer 5 of J-II central and Layer 5 onward of JT square, the cultural layer from which pottery was recovered, so it is clear that stone vessels continued to be used after the introduction of pottery at Charmo.

Pottery-related objects of interest were also recovered. Two clay vessels (Figs. 6-2-1 and 6-2-2) were discovered in the snail layer of Layer 9. They are very small objects made of unfired

clay, and it is unclear whether they served as vessels given their size and shape. There were no similarities in size or shape among the pottery discovered in large numbers in JT square Layers 4 and above. An additional small sandstone vessel excavated from Layer 6 is interesting. Its interior and exterior surfaces are covered with yellow slip, as is done on pottery (Fig. 6-3). Although it is a small fragment, it may indicate that stone vessels were sometimes decorated like pottery.

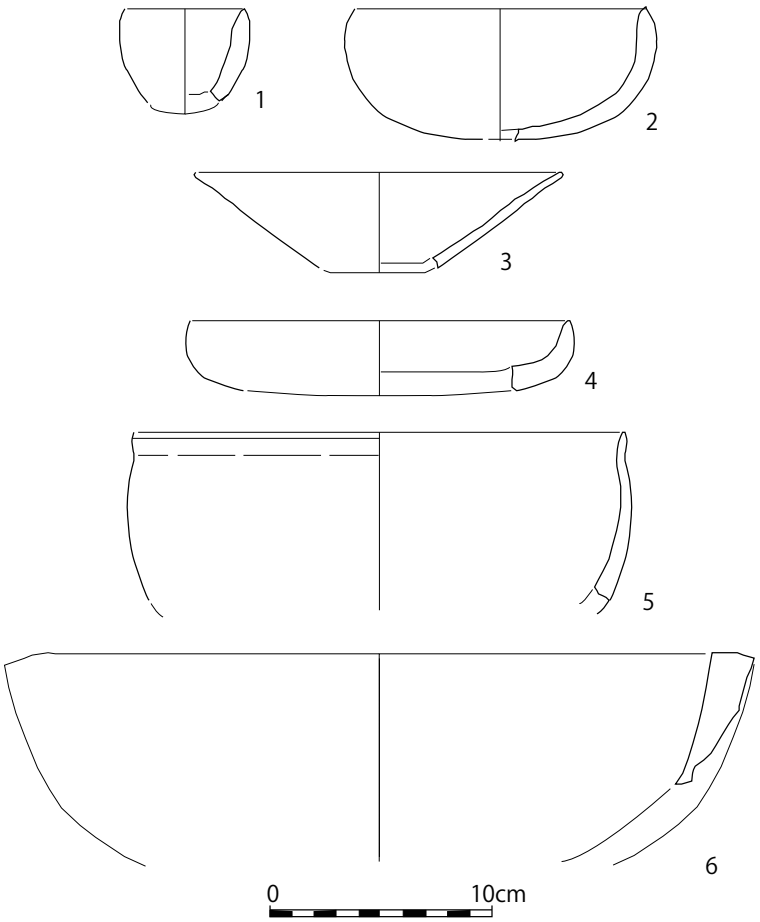

Fig. 6-1 Stone vessels made of marble (1-3) and sandstone (4-6).

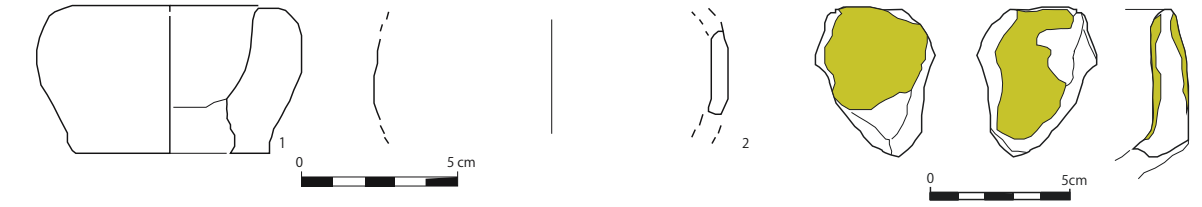

Fig. 6-2 Clay vessels in Layer 9.

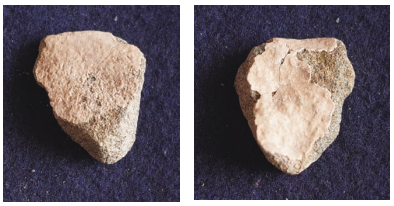

Fig. 6-3 Sandstone vessel covered with yellow slip discovered in Layer 6.

Bone implements

A beautiful bone-spoon was unearthed in Layer 7 (Fig. 6-4). It is similar in size and shape to previously excavated marble spoons but exhibits a more delicate construction. The tip of the handle is cut at an angle and incised. At least 11 other bone implements, including awls, needles, and spatulas, were also discovered (Fig. 6-5).

Stone axes

Five stone axes were found in Layer 10 in close proximity (Figs. 6-6 and 6-7). The materials were serpentinite and chert with beautiful finishes. The largest stone axe (Fig. 6-7) was the most notable, with a bitumen-like material remaining on the front and back where the handle was attached to the opposite side of the blade. Scientific analysis of this material is currently underway. If it is bitumen, it will be an example of the use of bitumen as a handle anchoring material.

Ornaments

Marble bangles, marble and chert beads, and pearly shell pendants such as Unio were discovered (Fig. 6-8). Unfinished beads and other ornaments were unearthed, indicating that they were made in Charmo.

Chipped stone industry

A total of 1,345 pieces of chipped stone were discovered in the J-II central NW area during the 2023 season. Of these, 971 were flint and 374 were obsidian. The flints included natural flint stone, primary cores, blade cores, flake cores, core preparation flakes, and microblade cores, which clearly indicates that blade production took place within Charmo village, including sickle elements, scrapers, burins, notches, points, and drills, all of which were few in number. There were a significant number of truncated and retouched blades;

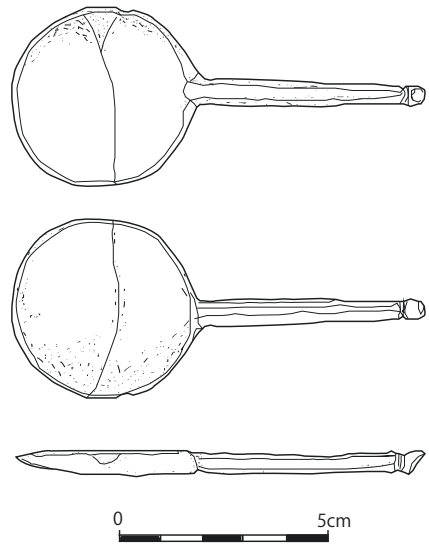

Fig. 6-4 A beautiful bone-spoon unearthed in Layer 6.

Fig. 6-5 Various bone implements.

Fig. 6-6 Stone axes unearthed in Layer 10.

Fig. 6-7 Stone axe with traces of bitumen unearthed in Layer 10.

Fig. 6-8 Various ornaments made of marble, chert and shell.

therefore, it is likely that these were sickle elements, but most of them lacked a sickle sheen. Even among the blades that can be classified as sickle elements, there were many examples in which the sickle sheen was very thin. I cannot determine whether the reason for this is the harvesting method or if harvesting itself was not performed very often.

As far as obsidian is concerned, 15 blades and 296 microblades were counted, but only 2 obsidian cores and 4 core preparation flakes were found, making them rare. If obsidian production took place in Charmo village, it was minimal, and most of the obsidian was probably brought to the village in its product form. Tools included notches, drills, and scrapers; however, only a few were found. Therefore, we can assume that obsidian tools were used as microblades. Two obsidian side-brow blade flakes were discovered.

Mats woven with reeds

Following last season's excavations at J-II central, many fragments of mats woven with reeds have been unearthed in this seasons' investigation. If even the smallest fragments are counted, the number of pieces is in the dozens. However, approximately only 10 good and beautiful remaining mats larger than 10 × 10 cm square exist in total. One mat each from Layers 7–9 and seven from Layer 10 were excavated. These mats are made by weaving reeds into a meshwork, which remains carbonized (Fig. 6-9). In the Braidwood investigations, examples of "reed flooring" left covering the floors of buildings have been identified, including J-I operation level 6 and J-II operation level 5 [Braidwood *et al*. 1983: Fig. 41 and Fig. 51]. In our example, whether these are mats on the floor or part of the ceiling material is not clear, although they appear to be basically similar.

We can propose three candidates for the materials of these carbonized mats discovered at Charmo. All are water reeds and straws that grow alongside of the *kani* water near Charmo. They are *Hasir*, *Zhash*, and *Qamish* (Fig. 6-10) in the local language. After comparing modern specimens with carbonized mats, we temporally concluded that the mats were woven by loosening and beating *Qamish* stems (Fig. 6-11). The scientific name of *Qamish* seems to be *Phragmites karka* (Retz.). *Qamish* stems are often used as ceiling material in modern Kanisard village. As *Qamish* grows relatively tall, it is often planted in the courtyards of houses in the Kanisard village to provide

shade. *Qamish* might have been also planted in Neolithic Charmo houses, and likely used as part of the building material.

Fig. 6-9 Mats woven with reeds.

Fig. 6-10 Candidates for the material of mats (left: *Hasir*, middle: *Zhash*, and right: *Qamish*).

Fig. 6-12 Set of quern and ground stone found in Layer 10.

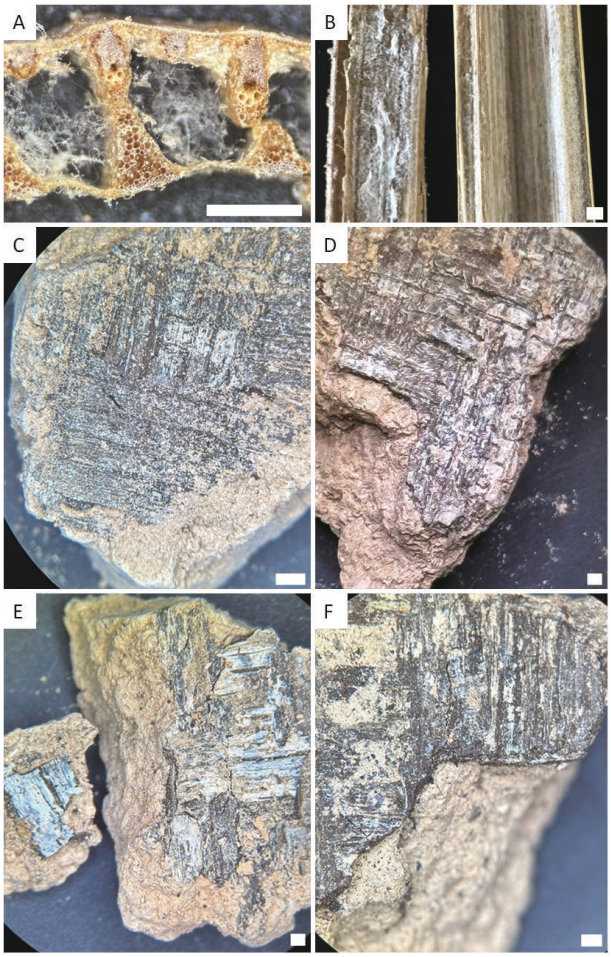

Fig. 6-11 A: Cross section of stem of modern *Qamish*, B: Inside of stem of modern *Qamish*, C: Mat fragment from Layer 7, D.F: Mat fragments from Layer 8, E: No. 4 Mat from Layer 10 (Photos by S. Tsuneki).

Querns and ground stones

In Layer 10, a large quern was unearthed, as well as a ground stone nearby (Fig. 6-12). Although only a small number of these tools have been excavated, these tools were likely used to grind wheat into flour.

(Akira Tsuneki)

7. Obsidian stratigraphy of the Charmo J-II central square

To establish an obsidian stratigraphy from the Charmo site, we performed chemical compositional analyses of the obsidian tools excavated from the J-II central square deepened during the spring-summer 2023 season, based on *in-situ* X-ray fluorescence spectrometer (XRF) data. We used an Olympus VANTA VCR-CCC (Rh target, 4 W X-ray tube) portable XRF and allocated 30 s to Beam 1 (at an accelerating voltage of 40 kV to measure the concentrations of Ti, V, Cr, Mn, and 23 elements heavier than Fe) and 60 s to Beam 2 X-ray irradiations (to measure Mg, Al, Si, P, S, K, Ca, Ti, and Mn at an acceleration voltage of 10 kV). The reliability of these measurements was evaluated by measuring a set of standard rock-slab samples with known concentrations of each element (Anma *et al.*, 2023). Based on repeated analyses of the rock-slab standards, the concentrations of Al, K, Ca, Ti, Mn, Fe, Zn, Rb, Sr, Y, and Zr with good correlations between the measured and recommended values were confirmed to be reliable and used for further consideration. The average LE (total amount of elements lighter than Na) of 66 repeated measurements performed on the flat surfaces of standard Shirataki obsidian slabs was ~56%.

We analyzed 391 obsidian tools excavated from Layer 6 to Layer 11 of the J-II central square NW area during the 2023 field season. To minimize the errors in the analytical values due to thickness and surface conditions (*e.g.* surface irregularity and roughness) of the samples, the analytical values were evaluated when LE fell within the range between 58% and 45%. In total, 297 obsidian data were within this range out of the total 391 data sets. Al and Ca data were not used for the current analyses because their measurements tended to be influenced by the thickness and surface conditions when compared with heavier elements.

Together with 216 obsidian data collected during the 2022 field season from Layers 5 and 6 of the J-II central square, 513 obsidian data were plotted on the Sr-Zr diagram (Fig. 7-1 left). In the diagram, the measured obsidian tools can be broadly divided into three groups: Group I with Zr concentrations of 200 to 300 ppm and Sr concentrations of approximately 50 ppm; Group II with Zr concentrations of over 1,000 ppm and no Sr, with two exceptions from Layer 6, which contain a few ppm Sr; and Group III, which contains ~15 ppm Sr and ~200 ppm Zr.

In the Rb/Zr-Fe/Mn diagram (Fig. 7-1 right), Group II obsidian samples can be divided into Group II-1, with Rb/Zr ratios below 0.19 and Group II-2 above 0.19. When comparing the Fe/Mn ratios of the J-II central square Group II-1 obsidian samples with those excavated from Layers 1 to 5 of the JT square of Charmo (Fig. 7-2) [Tsuneki *et al.*, 2023], it appears that Group II-1 obsidian

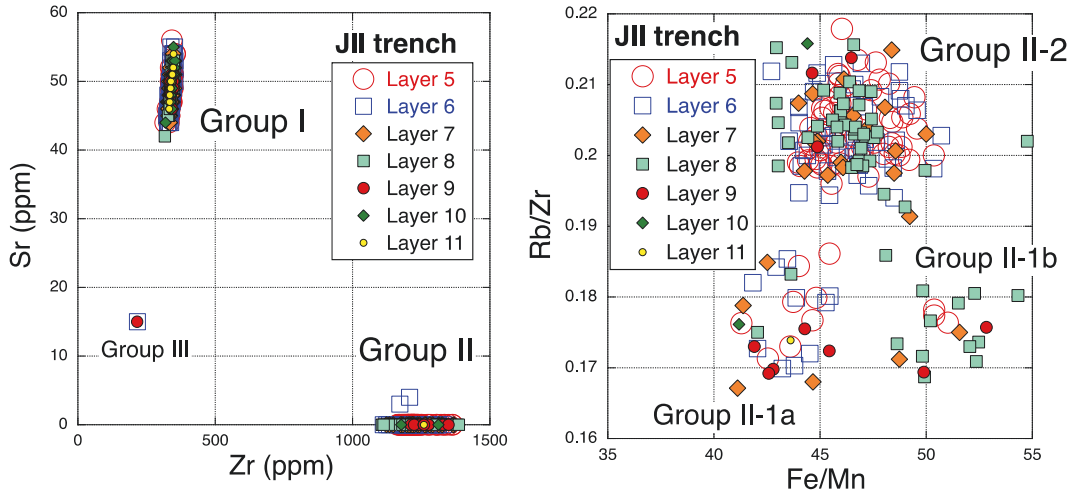

Fig. 7-1 Sr-Zr plot (left) and Rb/Zr-Fe/Mn plot (right) for the obsidian tools excavated from Layers 5 to 11 of the J-II central square during the 2022 and 2023 field seasons.

was more frequently used during the Layers 1 to 5 period of the JT square, whereas in the Layers 5 to 11 period of the J-II central square, Group II-2 obsidian was mostly used. The comparison further indicated that half of the J-II central Group II-1 obsidian tools (Group II-1b) had Fe/Mn ratios higher than 48, whereas this component was not significant in the JT square, and the majority (Group II-1a) had a lower Fe/Mn ratio (42–47).

The relative frequencies of these obsidian groups are listed in Table 7-1 for each stratigraphic horizon of the J-II central square together with the total number of appearances. The total number of obsidian tool appearances decreased with increasing depth from Layers 5 to 11. Table 7-1 and the relative frequency illustrated in Fig. 7-3

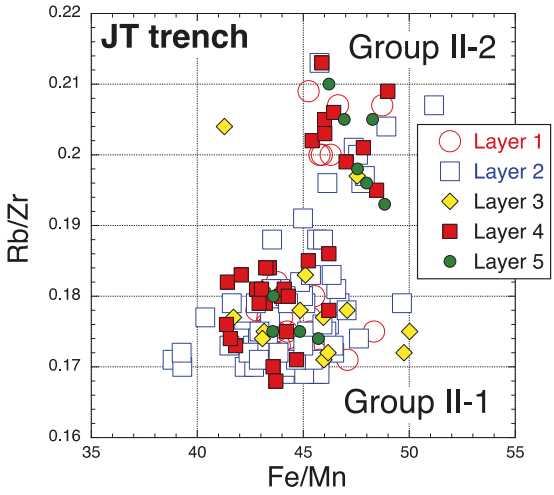

Fig. 7-2 Rb/Zr-Fe/Mn plot for the obsidian tools excavated from Layers 1 to 5 of the JT square during the 2022 field season.

Table 7-1 Classification of J-II central square obsidian groups based on geochemistry and their relative frequencies in % and number of appearances (in brackets) are indicated. Data from the 2022 and 2023 field seasons are included in the statistics.

JIIC trench	Group I	Group II-1a	Group II-1b	Group II-2	Group III	total
Layer 5	34% (35)	5% (5)	3% (3)	58% (59)	0% (0)	102
Layer 6	60% (86)	8% (11)	0% (0)	31% (45)	1% (1)	143
Layer 7	76% (78)	4% (4)	2% (2)	18% (19)	0% (0)	103
Layer 8	40% (37)	2% (2)	13% (12)	45% (42)	0% (0)	93
Layer 9	48% (10)	24% (5)	9% (2)	14% (3)	5% (1)	21
Layer 10	92% (23)	4% (1)	0% (0)	4% (1)	0% (0)	25
Layer 11	96% (25)	4% (1)	0% (0)	0% (0)	0% (0)	26

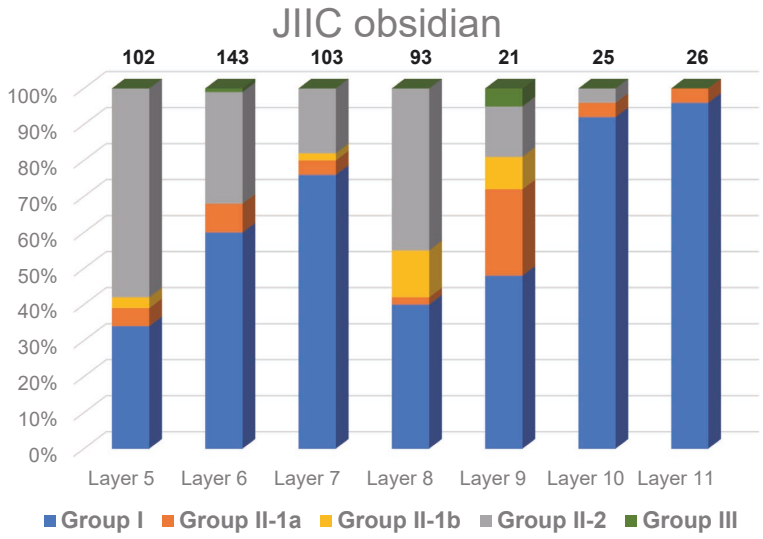

Fig. 7-3 Standard obsidian stratigraphy of the Charmo J-II central square established using the data set collected during the 2022 and 2023 field seasons.

indicate that Group I obsidian was mostly used in the lowermost Layers 10 and 11, whereas Layers 9 to 5, Group II-2 obsidian became more frequently used. The use of Group II-1 obsidian was not significant throughout these periods but did exist. Group III obsidian appeared only in Layers 6 and 9.

Previous studies by Maeda (2009), Frahm (2012), Chataigner and Gratuze (2014a, b), and Campbell and Healey (2016) showed that the Group I obsidian was most likely sourced at Bingöl B obsidian site, whereas Group II-1 and Group II-2 obsidians may be correlated with Nemrut Dağ and Bingöl A obsidian sites, respectively. Thus, throughout the late Pre-pottery Neolithic period, Bingöl B (Group I obsidian) was a major supplier of obsidian to the Jarmo site. Over time, but still during the PPN period, the Bingöl A (Group II-2 obsidian) producer won the position of the primary producer. Nemrut Dağ (Group II-1 obsidian) supplied obsidian to the Charmo site from the very beginning, but it was never a major supplier during the PPN period. Careful consideration of producers in Groups II-1b and III is necessary.

(Ryo Anma)

8. Ethnoarchaeological study on the *tannor* discovered during the 2022 season

During the 2021 excavation season, a very well preserved *tannor* (Str. 12) was detected externally on the west wall of Str. 10 in Layer 6 of the J-II central. As previously reported, the floor surface of the *tannor* is made of beautiful, blackened mud plaster, with a hole on the northern side for smoke exhaust or air vents (Fig. 8-1). Although parts of the walls of the *tannor* remained, it is unclear where the opening was located because the upper structure was not preserved. Braidwood [Braidwood *et al*. 1983] discovered a similar oven-like structure and *tannors* of this construction; however, the original use of this type of structure was not specified. Although it was highly likely a cooking facility, no carbonized material or other artifacts were recovered from *tannor*; therefore, it is unclear what type of cooking method was used.

In recent years, microscopic observation of food remains (carbonized cereals and other food products) has allowed us to establish a method for distinguishing cooking methods (*e.g.*, bread and porridge) [Fuller and Gonzalez Carretero, 2018]. Although further analysis of botanical remains and other artifacts discovered at the site is needed to make reasonable suggestions on the use of these structures, we conducted an ethnographic survey on modern *tandoor* in Kanisard, a village located near the site, to gather reference information. During the project period, we visited village residents' households to observe the structure and use of *tandoor*.

Tandoor (known as also "*Tannor*") is a pot-shaped or cylindrical earthenware oven with an opening at the top, commonly found in the countryside of the Middle East. *Tandoor* is commonly used for baking thin, disc-shaped loaves of bread that are eaten daily in the region. The structure of the *tandoor* varies regionally. They may be cylindrical, conical, or jar-shaped, with an opening at the top, and sometimes accompanied by a ventilation hole near the bottom. *Tandoors* with ventilation holes are common in modern Iraqi Kurdistan, including Kanisard.

In Kanisard village, each house has a

Fig. 8-1 3D image of *tannor* (Str. 12), discovered on the western wall of the Str. 10 building.

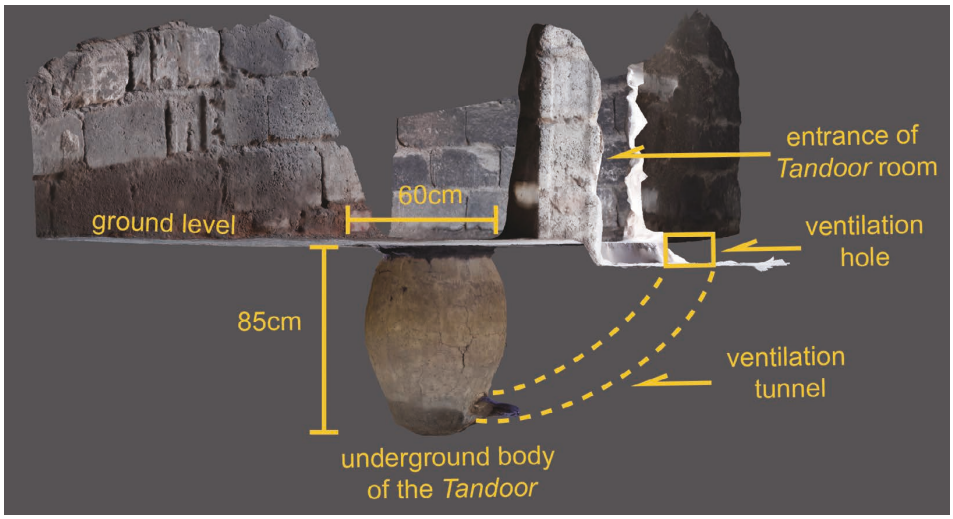

Fig. 8-2 3D image of modern *tandoor* at Kanisard village near Charmo.

small room in the courtyard for *tandoor* to bake disc-shaped flat thin bread for daily consumption. The *tandoor* that we observed was embedded underground and had a jar shape (Fig. 8-2). The interior was composed of clay. A ventilation tunnel used to adjust to the fire led to an opening hole in the wall of the *tandoor*. The diameter of the opening of the tandoor was 60 cm and the depth was approximately 85 cm. Once the wood fuel placed at the bottom was heated, bread dough was quickly pasted onto the wall using a small cushion made of fabric.

The bread eaten in Iraqi Kurdistan is relatively thin; therefore, it takes only a few dozen seconds for one piece of bread to be baked (Fig. 8-3). The fuel and ash are placed inside and removed through the openings. The strength of the fire is adjusted by opening and closing the ventilation hole that emerges from the ground. Because the structure of the *tandoor* room is not airtight and has vents on the wall, it appears that the smoke from the tandoor does not fill the inside of the room.

Fig. 8-3 Baking bread.

Conclusion

Observations of tandoor in the village of Kanisard were useful for understanding the variations in ancient and modern fireplaces and food preparation techniques. The use of Str. 12 at Charmo is currently unclear; however, future regional comparative studies with similar fireplaces from other archaeological sites will be carried out, and ethnographic data will be collected to determine the type of consumed plants and animals, cooking-related activities, and tools excavated at Charmo.

(Mariko Makino)

9. Survey and preliminary reconstruction of the Neolithic land use around Charmo

The field survey

A survey around Charmo was conducted to clarify the distribution of artifacts. The purpose of the

survey was to understand the spatial patterns of human activity and to identify areas with minimum land surface erosion[1]. The survey was conducted on June 26, 27 and 29, 2023 by Watanabe and Jammo. Each surveyor used a hand-held GPS device to record both the tracklogs and positions of the artifacts. When several artifacts were continuously found within a certain spatial extent, we recorded them as one "location" with a representative coordinate. Tracklogs were used to distinguish the difference between the "no artifacts" and "haven't been surveyed" for the place where nothing was recorded. In addition, tracklogs were valuable in evaluating the probability of finding artifacts, as noted in the following section. The artifacts found in the survey were mostly stone tools (Fig. 9-1). Not only the stone tools, but also artifacts such as bricks and pottery sherds were found. Most stone tools seem to be from the Neolithic Period. It is noteworthy that no single stone tools made from obsidian, which can be found in Chramo, were found in the survey. In addition, a stone tool with sickle gloss was collected approximately 700 m north from the center of Charmo (Fig. 9-2), which is considered in the following section.

Summarizing the results of the field survey

A grid consisting of squares with a resolution of 50 m was used to evaluate field survey results. Tracklog points (recorded every 1 s) within a unit square were counted to roughly calculate the amount of time spent inside the squares[2] (Fig. 9-3). The results show that the survey in 2023 covers a 1 km radius of Charmo when aggregated with the survey conducted in 2022 (2022/9/3–9/6, 9/18). The stone tools found in both surveys were integrated and counted within square units, as shown in Fig. 9-4. Fig. 9-5 shows the overlay of "walkedness" (Fig. 9-3) and the index representing the chance of stone tools to be detected (number of stone tools/walkedness). This index is intended to balance the detection of stone tools. For example, even if many artifacts are found, if

Fig. 9-1 Example of the artifacts found in the survey.

Fig. 9-2 Stone tool with sickle gloss (see Fig. 9-4 for the location of collection).

1) A location where artifacts are discovered can be regarded as land that has not undergone severe erosion and is expected to preserve its original land surface. Of course, there can be an inflow of artifacts originating from higher lands. However, many of the artifacts were found near the ridge-shaped topography, which still can be close to the original position. This information is used for reconstructing the landscape, which is one of our future goals.

2) Time can increase not only by just searching for artifacts, but by packing collected artifacts or due to the steep topography that takes longer time to walk through. However, staying time tends to be longer at the place where more artifacts are found.

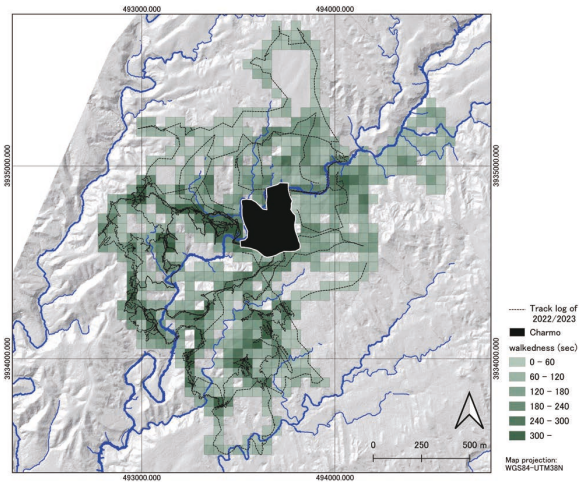

Fig. 9-3 Tracklog of the surveys in 2022 and 2023 overlaid with the "walkedness" (The time spent within the square unit) for the square unit of 50 m resolution.

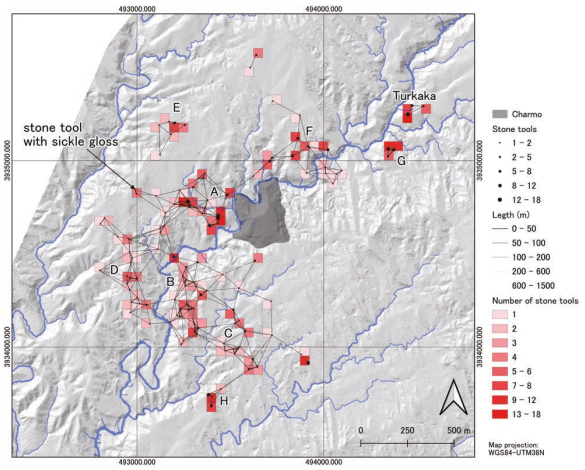

Fig. 9-4 Location of stone tools found, connection among the found locations, and number of the stone tools within the square unit of 50 m resolution (from the 2022 and 2023 surveys). Several clusters of points where stone tools were densely found can be assumed (*i.e.*, "A" to "H" in the figure).

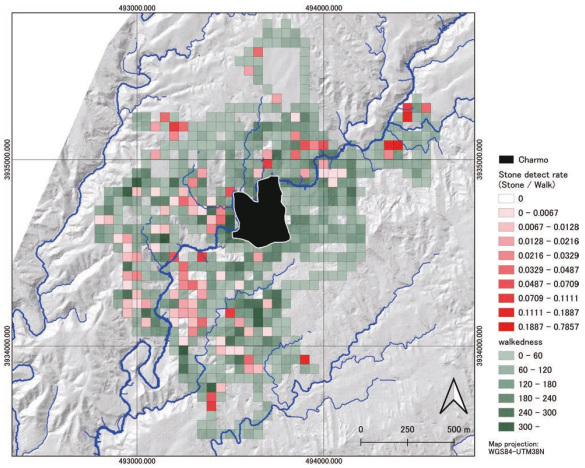

Fig. 9-5 Overlay of a probability of detection of stone tools (Number of stone tools/ walkedness) and "walkedness". This figure comprehensively shows the concentration and absence of stone tools around Charmo with the correction of the "walkedness".

the time spent there is long, the calculated value for this index will be lower. Thus, a mesh with "high walkedness" and "no findings" implies that it is highly probable that there are no artifacts in the area, whereas "low walkedness" and "many findings" imply a concentration of artifacts in the area. The bias was minimized by calculating the ratio of the number of stone tools to the time spent in the square unit. There seems to be no considerable bias in Fig. 9-4 because the tendency in Fig. 9-4 and 9-5 is correlative (values in squares around area A are moderated in Fig. 9-5, but still comparatively high). To gain a basic idea of the connection between the points and the structure of their clusters, the network and distances were calculated based on the Triangulated Irregular Network (TIN) ("length" in Fig. 9-4). The scale of the cluster differs according to the threshold length; thus, this is only a preliminary attempt to consider the grouping of the points. It was not clearly dividable but the points were roughly clustered and divided into "A" to "H" (Fig. 9-4). The clustered areas were comparatively concentrated on the western side of Charmo. Especially, "A" can be most strongly related to Charmo, considering the distance and the density of stone tools. However, it cannot be continuous with Charmo, because obsidian tools were found only in Charmo. To understand the relation of "A" and Charmo, the condition of Cham Gawra, the wadi flowing between them, needs to be considered as well. "B," on the same bank of Cham Gawra, is also an area comparatively close to Charmo where stone tools were densely found. However, there is a gap of absent area between "B" and Charmo, which again, indicates that it is not a continuation of Charmo. "E," "G," and "H" are distanced from Charmo,

which may not be directly related. Thus, the zone including "A" to "C" and "F" where the stone tools were densely found and close to Charmo, could be an area actively used on a daily basis. In summary, obsidian tools were not found outside Charmo; thus, these areas can be considered off-site of Charmo. On the other hand, one stone tool with sickle gloss was found in the survey (Fig. 9-2). However, this tool does not take the form of a typical sickle element. In addition, the glossy part is at the point of the tool and its area is small. Further analysis (*e.g*. confocal scanning microscopy [F. Pichon *et al*. 2023]) can be conducted to understand its usage, but it is likely related to agricultural activity, perhaps for husking. The tool was found in an isolated place where the topography is flat and different from that of the zone mentioned above (Fig. 9-4). It is difficult to make a conclusion from a single stone tool, but perhaps, this can be related to the preference toward the selection of agricultural land.

(Nobuya Watanabe)

10. ^{14}C data from the 2022 season

Method

Charcoal samples were pretreated using an acid/alkali/acid treatment [de Vries and Barendsen 1954]. Briefly, 2 mg of charcoal (containing 1 mg of carbon) was purified by chemical treatment and combusted using an elemental analyzer (Vario ISOTOPE SELECT, Elementar) at the University Museum, University of Tokyo [Omori *et al*. 2017]. Graphite was then produced by the catalytic reduction of CO_2 with iron powder [Kitagawa *et al*. 1993]. The radiocarbon content of the graphite was measured using an accelerator mass spectrometer (AMS) at the University Museum, University of Tokyo (Lab. code TKA-). Radiocarbon dates were statistically analyzed and calibrated using OxCal [Bronk Ramsey 2009] and IntCal20 calibration data [Reimer *et al*. 2020].

Table 10-1 Results of the radiocarbon dating for charcoal samples from Charmo.

Area	Sample No.	Layer	δ^{13}C	calibration curve	Lab. No.	^{14}C age (BP)	calibrated BC (1σ)	calibrated BC (2σ)
JII central	No. 5	Layer 5	–25.5 ± 0.2	IntCal20	TKA-26873	7970 ± 25	7035–6825	7040–6700
JII central	No. 6	Layer 5	–25.9 ± 0.3	IntCal20	TKA-26874	7930 ± 25	6910–6695	7030–6655
JII central	No. 7	Layer 5	–25.9 ± 0.2	IntCal20	TKA-26875	7945 ± 25	7025–6700	7035–6695
JII central	No. 8	Layer 5	–26.4 ± 0.3	IntCal20	TKA-26876	7890 ± 25	6775–6650	7020–6645
JII central	No. 10	Layer 6	–25.2 ± 0.3	IntCal20	TKA-26877	7940 ± 25	7025–6700	7035–6690
JII central	No. 16	Layer 6	–25.9 ± 0.2	IntCal20	TKA-26878	7965 ± 25	7035–6780	7040–6700
JII central	No. 23	Layer 5	–29.4 ± 0.2		TKA-26879	N.D.	dead	dead
JII central	No. 24	Layer 5	–26.1 ± 0.3	IntCal20	TKA-26880	7965 ± 25	7035–6780	7040–6700
JII central	No. 26	Layer 6	–26.2 ± 0.3	IntCal20	TKA-26881	7965 ± 25	7035–6780	7040–6700
JII central	No. 27	Layer 6	–26.7 ± 0.2	IntCal20	TKA-26882	8000 ± 25	7045–6830	7050–6775
JII central	No. 28	Layer 6	–27.6 ± 0.3	IntCal20	TKA-26883	7985 ± 25	7040–6830	7045–6705
JII central	No. 29	Layer 6	–24.3 ± 0.3	IntCal20	TKA-26884	7910 ± 25	6820–6690	7025–6650
JII central	No. 30	Layer 6	–25.3 ± 0.2	IntCal20	TKA-26885	8060 ± 25	7070–6865	7130–6830
JII central	No. 31	Layer 6	–26.4 ± 0.3	IntCal20	TKA-26886	29500 ± 95	32310–32035	32410–31870
JT	No. 9	Layer 4	–25.7 ± 0.2	IntCal20	TKA-26887	7750 ± 25	6640–6510	6645–6500
JT	No. 11	Layer 5	–26.1 ± 0.3	IntCal20	TKA-26888	7650 ± 25	6500–6450	6570–6435
JT	No. 13	Layer 5	–21.5 ± 0.3	IntCal20	TKA-26889	7800 ± 25	6650–6600	6690–6570
JT	No. 15	Layer 4	–24.7 ± 0.2	IntCal20	TKA-26890	7790 ± 25	6645–6595	6685–6515
JT	No. 17	Layer 5	–28.7 ± 0.2	IntCal20	TKA-26891	7730 ± 25	6595–6505	6640–6475
JT	No. 18	Layer 5	–24.2 ± 0.3	IntCal20	TKA-26892	7760 ± 25	6640–6540	6645–6505
JT	No. 21	Layer 5	–28.5 ± 0.3	IntCal20	TKA-26893	7700 ± 25	6570–6475	6595–6470

Result

Twenty-two charcoal samples from Charmo, 14 from the J-II central square, and 8 from the JT square were treated with AAA, of which 21 samples yielded the amount needed for AMS measurement. These 21 samples were prepared for graphitization, and their radiocarbon isotope ratios were determined (Table 10-1).

Twelve of the samples from J-II central were dated from 7070 cal BC to 6700 cal BC, giving an overall date from the end of the eighth millennium BC to the first quarter of the seventh millennium BC (Table 10-1, Fig. 10-1). In contrast, two objects from J-II central showed low radiocarbon concentrations of ca. 30,000 BP or below the detection limits, suggesting that these were petroleum-composed materials with dead carbon. In a previous excavation of the site, some specimens and pottery deposits that were likely bitumen were found, thus it is highly possible that these fragments were also bitumen.

The seven samples from the JT square showed dates from 6650 cal BC to 6450 cal BC, representing the middle of the seventh millennium BC. Layers 4 and 5 of the JT square are considered to belong to a relatively newer occupation layer than Layers 5 and 6 of J-II central.

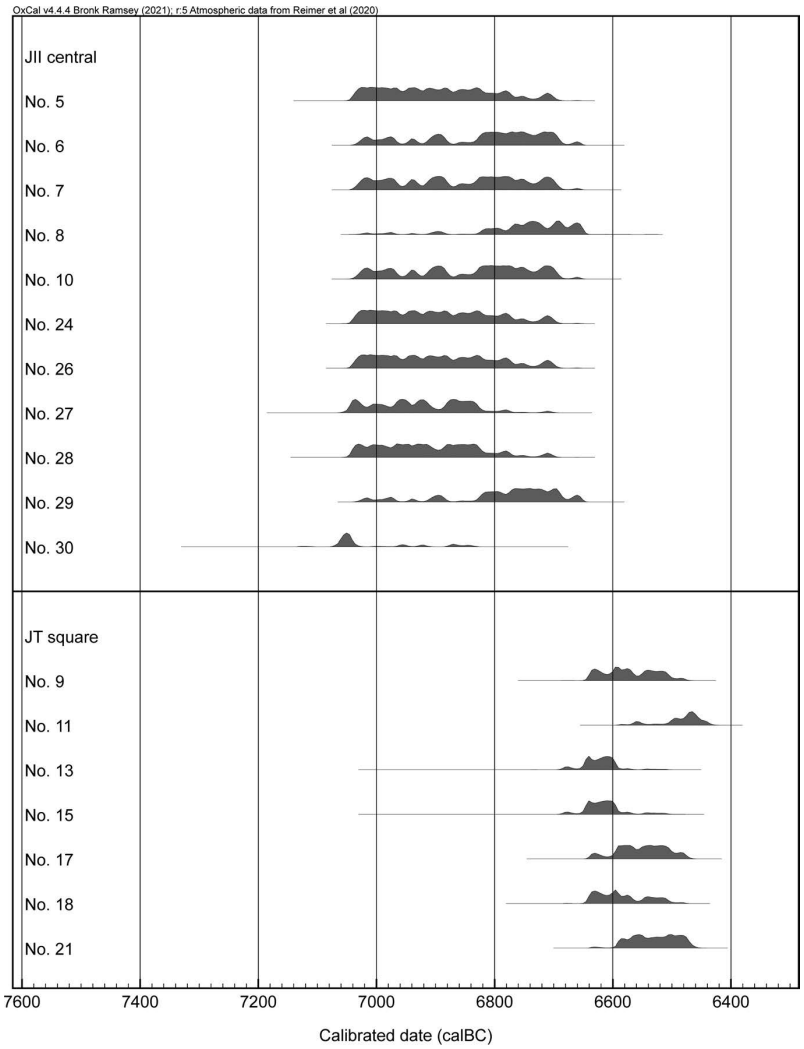

Fig. 10-1 Calibrated dates for charcoal samples from the J-II central and JT squares in Charmo.

(Yu Itahashi and Minoru Yoneda)

11. Bitumen resources in Slemani area

Excavations in the Middle East have revealed that natural bitumen resources are widespread in the Middle East. The population of this area, in particular, in the Zagros Mountains and its flanks and Mesopotamia, starting from prehistoric Neanderthal people, used bitumen as hafting material to fix handles of their flint tools. Natural bitumen and its role from the Neolithic period became more important and served to waterproof containers (baskets, earthenware jars, storage pits), wooden posts, palace grounds (*e.g.*, in Mari and Haradum), reserves of lustral waters, bathrooms, palm roofs, mats, sarcophagi, coffins, and jars used for funeral practices. These objects were often covered and sealed with bitumen. Bitumen was also a widespread adhesive in antiquity and served to repair broken ceramics and fix eyes and horns on statues (*e.g.*, at Tell al-Ubaid around 2500 BC). Beautiful decorations with stones, shells, mothers of pearls, palm trees, cups, ostrich eggs, musical instruments, and other items such as rings, jewelry, and games were excavated from the royal tombs in Ur [Connan 1999: 33].

Bitumen was unearthed during archaeological excavations in Mesopotamia, in sites such as Tell al-Ubaid (around 2500 BC), royal tombs in Ur, Susa, and Tell el 'Oueili (5800–3500 BC). In antiquity, there were two ways to obtain bitumen from trade; the first was a close distance of less than 50 km, and the second was long-distance trade starting from 50 km.

In Charmo, we found many potsherds with traces of bitumen on them during the 2019 sounding excavations (Fig. 11-1). For this reason, Prof. Akira Tsuneki asked me to conduct surveys to find bitumen resources in all Slemani regions, from Halabja in the east to Chamchamal in the west. The aim of the surveys was to identify bitumen sources and compare them with ones Charmo people used in their time. Accordingly, we asked our guard-watchers in all regions of the Slemani Directorate of Antiquities about the bitumen sources.

Fig. 11-1 Potsherds from Charmo with traces of asphalt.

Finally, we were informed about the two directions in which we could find sources. The first is in the Chamchamal area, approximately 40 km northwest of Charmo, and the name of the source is Qirina (Fig. 11-2). The second one is in the south of the Halabje area in

GPS: 36°44′35″N 44°47′51″E 2330 feet asl.

Fig. 11-2 Qirina source near Tlian village (Qirina bitumen).


GPS: 35°8′42″N 45°51′12″E 2230 ft asl.

Fig. 11-3 Pirg source in Shahrizor and a piece of bitumen.

Shameran, and the source is located in a village called Pirg (Fig. 11-3)

The areas of the two sources are completely different in terms of topographical and bitumen conditions. The Qirina source in Chamchamal has only a small mound with a wady valley and its bitumen is more liquid than the Pirg bitumen. Pirg in the Shameran area is a mountainous and hilly region covered with oak trees. The bitumen from this source is drier and harder (Fig. 11-3).

According to what we said above regarding trade distance, people from Charmo could obtain their bitumen from the Qirina source or other sources in the Chamachamal area, where we could not find it. Qirina is close to Charmo, at approximately 30 km, but Pirg in Halabja is far from Charmo, at approximately 100 km.

(Saber Ahmed Saber)

12. Insights into carbonaceous materials on pottery sherds: Raman spectroscopy at the Charmo archaeological site

Introduction

Carbonaceous materials within geological strata and rocks undergo various structural and chemical transformations during diagenesis and metamorphism, driven by variations in temperature and pressure. Raman spectroscopy emerges as a valuable tool for monitoring these structural changes, allowing for the identification of substances based on characteristics such as functional groups, chemical bonding, and structural order at the atomic scale [Jehlička *et al*. 2003]. Laser Raman microscopic spectroscopy, in particular, enables non-destructive characterization of miniscule amounts of carbonaceous matter, even those less than 2 microns in size [Pironon *et al*. 1991]. Consequently, this technique has found widespread application in the identification of kerogen, bitumen, graphite, diamond, and other constituents within rocks and geological formations. Moreover, it facilitates the determination of intermediate states associated with material changes and plays a crucial role in assessing maturity of oil and natural gas [Orange *et al*. 1996; Beyssac *et al*. 2002, 2003; Jehlička *et al*. 2003; Zhang *et al*. 2007].

In Raman measurements, a sample is irradiated with a monochromatic laser beam and the scattered Raman light is then separated and measured by wavelength. However, when analyzing substances prone to fluorescence under laser irradiation, the measurement process can be challenging due to the masking effect of the fluorescence background on the Raman scattered light [Pironon *et al*. 1991; Zhou *et al*. 2014]. In particular, organic samples containing aromatics are often difficult to measure due to the generation of fluorescence [Pironon *et al*. 1991; Orange *et al.* 1996]. Photodegradation of the sample due to laser irradiation may be problematic (Jehlička *et al*. 2003).

These challenges, however, can often be mitigated by significantly reducing the intensity of the irradiating laser beam or by carefully selecting the wavelength of the beam for measurement (Orange *et al*. 1996), coupled with the implementation of a suitable background subtraction technique (Khatibi *et al*. 2019). In the context of this study, Raman measurements were conducted with a very weak beam irradiation to identify carbonaceous materials adhering to the potsherds.

Sample and method

The samples under investigation consisted of black materials adhering to two pottery sherds (IRCM-32-2 and 450) from Layer 6 of the J-II S trench at the Charmo site [Tsuneki *et al*. 2023]. The potsherds themselves exhibit a light brown to white color and are relatively brittle in nature. Notably, a thin layer of the black material was found adhering to the inner surface of the pottery (Fig. 12-1a). The surface of the black material displays grooves, resembling marks left by a thin comb (Fig. 12-1b). Upon examination, the cross sections of the black materials were found to be dark brown, dry, brittle, and earthy in texture. A previous report suggested that these black materials could be classified as a carbonaceous material with carbon-14 age exceeding 40,000 years, possibly bitumen [Tsuneki *et al*. 2023]. Bitumen, a material with a history of use dating back to 40,000 B.C., has served various purposes such as a mortar for construction, waterproofing agent, adhesive, and more [Connan, 1999]. Moreover, it is abundantly distributed in the Kirkuk region adjacent to the Charmo site [Connan, 1999]. In the present study, small portions (0.5 mm in size) of the black materials were collected from the two potsherds and subsequently mounted on slide glass as specimens.

Raman spectra of the specimens were measured using a confocal inVia Raman spectrometer (Renishaw, Wotton−under−Edge, UK) at the University of Tsukuba, Tsukuba, Japan. The measurements were performed at room temperature using a 532 nm (green) laser, which was focused through a 100 × microscope objective. The laser boasts a spatial resolution of approximately 1 μm. The spectral range covered by the samples extended from 50 to 4280 cm^{-1} wavenumber shift, with a spectral resolution of 4 cm^{-1}. The laser power was maintained at approximately 0.6 mW on the sample surface, and each spectrum was obtained with a 1 s acquisition time, accumulating 60 times, resulting in a total energy deposition of 0.6 mW.s onto the sample surface. To ensure spectral precision and consistent measurement conditions, calibration was performed before data acquisition using the 520.5 cm^{-1} Raman band of a silicon reference sample. In an effort to eliminate potential fluorescence background effects in the Raman spectra, a fifth-order polynomial baseline curve was fitted to the whole spectrum, and subsequently subtracted from the measured spectrum.

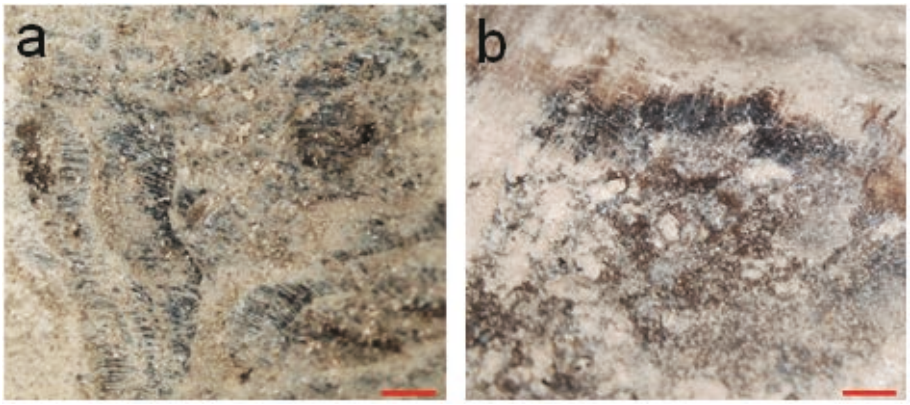

Fig. 12-1 Photographs of black materials adhering to potsherds from the Charmo site. (a) Sample IRCM-32-2. (b) Sample 450. Dark brown color represents carbonaceous materials. Scale bars are 1 mm.

Results and discussion

The first-order Raman spectra of the two black materials revealed a broad band spanning from 1380 to 1410 cm^{-1} and a wide band near 1600 cm^{-1} (Fig. 12-2a, b). In this spectral range, vibration bands associated with carbons within polyaromatic structures in carbonaceous materials become apparent [Beyssac *et al*. 2002, 2003]. Specifically, the band located at around 1580 cm^{-1} is assigned to the in-plane vibration of aromatic carbons in the polyaromatic structure, such as graphite, commonly referred to as the G (graphitic) band [Beyssac *et al*. 2002, 2003]. Concurrently, the band at around 1350 cm^{-1} is linked to defects or disordered structures within the polyaromatic framework and is designated as the D1 (defect or disordered) band [Beyssac *et al*. 2002, 2003]. The D1 band tends to be intense and very wide in poorly ordered carbons, and the position and width of the D1 band bear a close relationship to the degree of structural ordering within the carbonaceous material [Beyssac *et al*. 2002, 2003]. In perfectly crystalline carbonaceous materials such as graphite, only the G band is observed [Beyssac *et al*. 2002, 2003]. However, most disordered carbonaceous materials, including kerogen, bitumen, hydrocarbon fluid, coal, and disordered graphite, exhibit both the D1 and G bands [Orange *et al*. 1996; Kelemen and Fang 2001; Jehlička *et al*. 2003; Schito *et al*. 2017]. In the case of disordered materials like bitumen, the D1 band is assigned to the ring stretch of bicyclic and higher aromatic hydrocarbons, while the broad G band is assigned to the C=C stretch of all aromatic and other unsaturated species [Shoute *et al*. 2002]. The pronounced appearance of the D band and the broad width of the G band in the spectra indicate a very weak structural organization [Jehlička *et al*. 2003]. These characteristics of a disordered structure are clearly evident in the present spectra (Fig. 12-2a, b).

In the range of ~2800–3100 cm^{-1}, a distinct set of bands is observable (Fig. 12-2a, b). In this interval, overtone scattering (2×1405 $cm^{-1} = 2810$ cm^{-1}, 2×1601 $cm^{-1} = 3202$ cm^{-1}) and combination scattering (1405 $cm^{-1} + 1601$ $cm^{-1} = 3006$ cm^{-1}) of the D and G bands appear. Notably, these bands exhibit considerable broadening with an increase in structural disorder [Jehlička *et al*., 2003]. In addition, symmetric and asymmetric stretching vibrations of methyl and methylene in alkanes and cycloalkanes manifest around 2900 cm^{-1} (~2850 cm^{-1} for CH_2 symmetric of cycloalkanes and alkane; ~2920 cm^{-1} for CH_2 antisymmetric of alkane; ~2940 cm^{-1} for CH_2 antisymmetric of cycloalkanes and CH_3 antisymmetric of alkane [Orange *et al*. 1996]). An additional noteworthy feature is a prominent peak at 3062 cm^{-1}, indicative of the presence of aromatic hydrocarbons, including benzene and its derivatives [Orange *et al*. 1996].

The aforementioned features, consistently observed in the Raman spectra of natural bitumen (as exemplified in Fig. 12-2c), serve as reliable indicators for bitumen identification [Orange *et al*. 1996; Shoute *et al*. 2002;

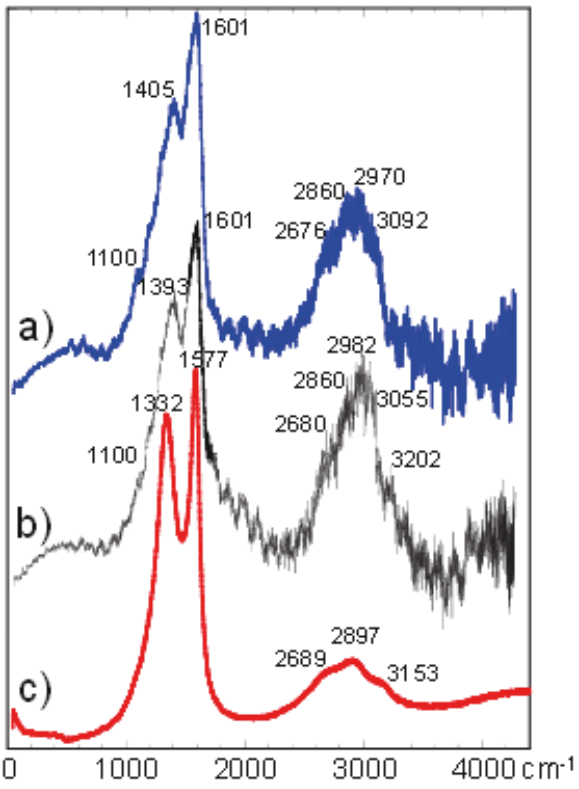

Fig. 12-2 Raman spectra of black materials adhering to potsherds from the Charmo site. The vertical axis represents intensity, and the horizontal axis represents Raman shift (cm^{-1}). (a) Sample IRCM-32-2. (b) Sample 450. (c) Natural bitumen in Cretaceous Torinosu limestone from Kochi, Japan [Kido *et al*., 2023].

Jehlička *et al*. 2003]. Thus, the black materials presented in Fig. 12-2a, b are confidently identified as bitumen. A comparison with natural bitumen found in Cretaceous limestone in Japan (Fig. 12-2c) reveals a shift in the D band position towards lower wavenumbers, and the distance between the D and G bands is wider compared to the black materials (Fig. 12-2a, b). The separation of the D-G band positions is known to increase with the rising thermal cracking (maturity) of carbonaceous materials [Kelemen and Fang 2001]. These shifts and changes are attributed to an increase in larger aromatic clusters and a better ordered-structure of kerogen in terms of the existing organic compounds [Schito *et al*. 2017]. Hence, the black materials under investigation are deemed less mature than the Japanese bitumen. Changes in the position, width, and intensity of the D and G bands due to the thermal maturity may provide important clues into distinguishing the origin and provenance of bitumen. Future investigations aim to explore this further through a comparative analysis with natural bitumen from surrounding areas.

(Masanori Kurosawa and Kei Ikehata)

13. Conclusion

Our Charmo investigations could not be conducted in 2020 and 2021 because of the COVID-19 pandemic, which prevented us from executing large-scale field investigations. However, we were able to conduct full-scale field investigations in 2022 and 2023 and obtain significant results.

As previously mentioned, excavations had two main objectives. First, to determine the chronology of the Charmo village from its beginning to its end, and second, to elucidate its specific aspects. Regarding the first objective, a JT square investigation in 2022 revealed that the Charmo village ended by the late 7th millennium BC. on an absolute date, whereas life in the village ended at approximately the same time or earlier than the Proto-Hassuna period in northern Mesopotamia. Regarding the beginning of the Charmo-framing village, this season's investigations revealed that the village was established on the marl soil groundmass at an elevation of approximately 725 m asl, providing considerable materials for absolute and relative dating. Thus, we should be able to obtain a complete picture of Charmo's age and chronology in the next year.

We learned a great deal about the aspects of early farming villages in Charmo. During the 2022 investigation, we detected a square-planned habitation building with a *pisé* wall and a well-preserved *tannor* (bread oven) with a ventilation hole. Inside the habitation building, a small clay platform was built in which three animal clay figurines were found, and some type of ritual practice was performed. The locations of stone vessels and stone bowl production, as well as a set of beautiful marble bowls and spoons, were also discovered in the ash pit. During the 2023 excavations, *pisé* walls and many ash pits were detected, and several carbonized seed deposits were found between them. In addition, as many as 20,000 snail shells were excavated, mainly from Layer 9. Many animal bones were also discovered. These plant and animal bone remains will shed light on the type of livelihood practiced in the early farming villages at Charmo. Research has already begun on flora and fauna approved for scientific analysis. We will obtain the results of these analyses in the near future to learn more about Charmo's subsistence in detail. Of particular interest to me is a series of carbonized mats that were unearthed in the excavations during both the last season and this season. These mats were woven from a family comprising true grasses, such as *phragmites* or *typha*, which were grown along the waterside. These plants were obtained from the Cham Gawra River or springs near Charmo village. These plants could also be planted around dwellings, as we see today in the village of Kanisard near Charmo. In any case, plants certainly not dry framing ones were used in the Neolithic village at Charmo. This would be expected to reinforce that early farming at Charmo was not "simple rain-fed farming," as Braidwood asserted, but "more complicated farming using springs in the water reservoir area," which we claimed [Tsuneki *et al*.

2019].

The most notable artifacts recovered from the 2023 excavations were stone vessels and clay objects. More than 40 stone vessels and 80 clay objects were discovered. The stone vessels are composed of marble, limestone, and sandstone. The shapes of the vessels differ according to the stone material; marble and limestone were made into bowls of various shapes, while sandstone was often dish-shaped. A very beautiful bone spoon and other bone awls are also remarkable artifacts. No potsherds were discovered below Layer 6. The clay objects include human figurines, animal figurines, small and large clay balls, other geometric forms, fragments of clay vessels, and other various forms. The number of unbaked clay objects is large; apparently, these were ubiquitous objects within the village of Charmo. Unbaked clay objects were more abundant in the lower layers up to Layer 6, and clay objects appear to have played a more important role in the ancient times of Charmo.

In the 2023 season, the first distinct human grave was detected in Layer 11. This was a customary pit grave during the Neolithic period. The deceased was an older adult, probably male, buried in a tightly flexed position on the left side. It was found near the *pisé* wall, and judging from the partially remaining plaster floor surface, it was assumed that it might have been an underfloor burial in a dwelling. The adult human skeleton and other excavated human remains were authenticated by Ms. Yuko Miyauchi and Prof. Kirsi, O. Lorentz, who specialize in physical anthropology.

The *tannor* found in the 2022 season (Str. 12) was scrutinized by Ms. Mariko Makino and compared to ethnic cases such as Kanisard village. As a result, it is almost certain that the flue-like ventilation hole facility that continues to the north of the *tannor* is an oxygen intake facility.

Geomorphological and geochemical investigations around Charmo were conducted on an ongoing basis by our geologist, Prof. Ryo Amma, during both the 2022 and 2023 seasons. The purpose of these investigations was to reconstruct the paleoenvironment of Charmo at the time of its occupation and identify the provenance of excavated artifacts. For the former purpose, Ryo Amma set up several erosion measurement pins near the Charmo site to measure the rate of erosion currently occurring at Cham Gawar. Regarding the degree of erosion since last year, he obtained erosion rates ranging from none to ~1.5 mm/year. These steady efforts have been a major resource for the restoration of Charmo's paleoenvironment, dating back more than 9,000 years. Progress has also been made in identifying the origins of excavated artifacts, particularly obsidian stone tools.

Prof. Nobuya Watanabe's ongoing survey of off-sites around Charmo is also largely aimed at reconstructing the paleo-topography of the Neolithic settlement of Charmo. He used the SfM to make 3D measurements of Charmo to determine the topographic changes in recent years. In addition, he started off-site surveys around Charmo in 2022. In 2023, southwest and northeast areas were surveyed and 272 artifacts were found at 111 locations. Based on these data, he reconstructed a preliminary paleoenvironment around the Neolithic Charmo village. The most interesting aspect of his reconstruction of the paleo-topography of Charmo is that the difference in elevation between Charmo village and the Cham Gawra River was much smaller in the Neolithic period than it is today. Furthermore, numerous Neolithic artifacts from the northwest side of Cham Gawra were identified, strongly suggesting that the opposite bank of Cham Gawar was used for daily occupation in those days. In this season, one of such opposite bank off-sites produced a sickle element, indicating that the opposite hills were also used for farming fields.

Our Charmo investigations have made significant progress over the past two years. The absolute and relative chronology of the Charmo Neolithic village will be fully determinable based on the large number of ^{14}C samples collected during the 2022 and 2023 investigations. Considerable flora and fauna data are also available on the transition of subsistence from the beginning to the end of the village, and the results may help reconstruct a more complicated subsistence strategy of the

Charmo people. We can, thus, add new insights into the village lives of the Charmo people. Paleo-topography and paleo-environmental reconstructions explain why people chose Charmo as a site for early farming village formation. The time for revealing the reality of Charmo's early farming villages and their historical significance is rapidly approaching.

(Akira Tsuneki)

Acknowledgments

For the execution of the archaeological research campaign in Slemani of Iraqi-Kurdistan, we are deeply grateful to the General Director of Antiquities, Ministry of Municipality and Tourism, Kurdistan Regional Government–Iraq. We express our special gratitude to Mr. Kaifi Mustafa Ali, the General Director of Antiquities and Heritage, KRG, for his kind permission to conduct our investigations at Charmo. We are deeply grateful to Mr. Hussein Hama Gharib Hussein, the Director of the Slemani Antiquities and Heritage Directorate. He encouraged us to conduct prehistoric investigations at Charmo, one of the most important prehistoric sites in Kurdistan. We are also grateful to Mr. Nawshirwan Aziz Mohammed, the Director of the Archaeological Excavation of the Slemani Antiquities Directorate, for his consistent support of our work. We would like to thank Mr. Saber Ahmed Saber, a staff member of the Slemani Antiquities Directorate, for his kind instructions and for accompanying us in the field as a representative dispatched from the Slemani Antiquities Directorate. Mr. Fereidoun Fayaq supported our investigation as a driver sent by the Directorate. We express our thanks to the staff at the Slemani Antiquities Directorate and Slemani Museum, especially Mr. Hassim Hama Abdulla, Mr. Sami Jamil Aziz, Mrs. Niyan Nasir Hama Hassan, and Mr. Akam Omar. At Chamchamal, Mr. Abdelrahman Saber Mohammad, a keeper of Antiquities at Takia, ensured every convenience for us during our fieldwork at Charmo. We also wish to express our special thanks to the people of Takia town and Kanisard village near Charmo for their inestimable support of our research as workers and for their hospitality.

We received considerable support from the KRG and the Embassy of Japan in Iraq. I would like to express my deepest appreciation to His Excellency Futoshi Matsumoto, Ambassador of Japan, for visiting the Charmo site and for his encouragement. I would like to thank Mr. Tatsuoki Miyakawa, First Secretary, for his attention during the Ambassador's visit.

The identification of the plants and animals excavated at Charmo is being carried out with the help of Prof. Dorian Fuller, Dr. Marjan Mashkour, Dr. Hitomi Hongo and others. For the identification of the reed, we got the assistance of Dr. Shizuka Tsuneki. We would like our deepest gratitude to them all.

The field expedition at Charmo was conducted from May 15 to July 5, and we continued supplemental work in the field and material studies until July 14, 2023. Financial support for this research came from grants of the Japan Society for the Promotion of Science (JSPS), Grant-in Aid for Scientific Research (A) "Reconsideration of Jarmo: Neolithization in the Eastern Wing of the Fertile Crescent" (20H00020).

Bibliography

Anma, R., Sano, T., Shin, K.-C., Kon, Y. and Matsui, K.
2023 Preparations of rock slab standard materials for pXRF analyses, *Annual Report for the JSPS Project*, *The Essence of Urban Civilization–An Interdisciplinary Study of the Origin and Transformation of Ancient West Asian Cities* 5, 187–197.

Beyssac, O., Goffe, B., Chopin, C. and Rouzaud, J.
2002 Raman spectra of carbonaceous material in metasediments: A new geothermometer, *Journal of Metamorphic Geology* 20, 859–871.

Beyssac, O., Goffe, B., Petitet, J., Froigneux, E., Moreau, M. and Rouzaud, J.
2003 On the characterization of disordered and heterogeneous carbonaceous materials by Raman spectroscopy, *Spectrochimica Acta A* 59, 2267–2276.

Braidwood, L.S., Braidwood, R.J., Howe, B., Reed, C.A. and Watson, P.J.
1983 *Prehistoric Archaeology along the Zagros Flanks*, Oriental Institute Publications 105, University of Chicago, Chicago.

Braidwood, R.J. and Howe, B.
1960 *Prehistoric Investigations in Iraqi Kurdistan*, Studies in Ancient Oriental Civilization 31, University of Chicago, Chicago.

Bronk Ramsey, C.
2009 Bayesian analysis of radiocarbon dates, *Radiocarbon* 51(4), 337–360.

Buikstra, J.E. and Ubelaker, D.
1994 *Standards for Data Collection from Human Skeletal Remains*. Arkansas Archaeological Survey Research Series 44, Arkansas Archaeological Survey.

Fayetteville, Arkansas. Campbell, S. and Healey, H.
2016 Multiple sources: The pXRF analysis of obsidian from Kenan Tepe, S.E. Turkey, *Journal of Archaeological Science: Reports* 10, 377–389.

Carretero, L.G., Lucas, L., Stevens, C. and Fuller, D.Q.
2023 Investigating early agriculture, plant use and culinary practices at Neolithic Jarmo (Iraqi Kurdistan), *Journal of Archaeological Science: Report* 52, Article 104264.

Chataigner, C. and Gratuze, B.
2014a New data on the exploitation of obsidian in the southern Caucasus (Armenia, Georgia) and eastern Turkey, part 1: Source characterization, *Archaeometry* 56, 25–47.
2014b New data on the exploitation of obsidian in the southern Caucasus (Armenia, Georgia) and eastern Turkey, part 2: Obsidian procurement from the Upper Palaeolithic to the Late Bronze Age, *Archaeometry* 56, 48–69.

Connan, J.
1999 Use and trade of bitumen in antiquity and prehistory: Molecular archaeology reveals secrets of past civilizations, *Philosophical Transaction of Royal Society of London Series B* 354, 33–50.

Dahlberg, A.A.
1960 The dentition of the first agriculturists (Jarmo, Iraq), *American Journal of Physical Anthropology* 18(4), 243–256.

Frahm, E.
2012 Distinguishing Nemrut Dağ and Bingöl obsidians: Geochemical and landscape differences and the archaeological implications, *Journal of Archaeological Science* 39, 1436–1444.

Fuller, D. and Gonzalez Carretero, L.
2018 The archaeology of Neolithic cooking traditions: Archaeobotanical approaches to baking, boiling and fermenting, *Archaeology International* 21, 109–121.

Jehlička, J., Urban, O. and Pokorny, J.
2003 Raman spectroscopy of carbon and solid bitumens in sedimentary and metamorphic rocks, *Spectrochimica Acta Part A* 59, 2341–2352.

Kelemen, S. and Fang, H.
2001 Maturity trends in Raman spectra from kerogen and coal, *Energy Fuel* 15, 653–658.

Khatibi, S., Ostadhassana, M., Hackley, P., Tuschel, D., Abarghani, A. and Bubach, B.
2019 Understanding organic matter heterogeneity and maturation rate by Raman spectroscopy, *International Journal of Coal Geology* 206, 46–64.

Kido, T., Kurosawa, M. and Ikehata, K.
2023 Hydrocarbon fluid inclusions in authigenic quartz from the Torinosu limestone at Sakawa town, Kochi Prefecture, Japan, *Journal of Mineralogical and Petrological Sciences* 118, 5.

Kitagawa, H., Masuzawa, T, Nakamura, T. and Matsumoto, E.
1993 A batch preparation method for graphite targets with low background for AMS 14C measurements, *Radiocarbon* 35, 295–300.

Lovejoy, C.O.
1985 Dental wear in the Libben population: Its functional pattern and role in the determination of adult skeletal ge at death, *American Journal of Physical Anthropology* 68(1), 47–56.

Maeda, O.
2009 *The Materiality of Obsidian and the Practice of Obsidian Use in the Neolithic Near East*, Ph.D. thesis, University of Manchester.

Meindl, R.S. and Lovejoy, C.O.
1985 Ectocranial suture closure: A revised method for the determination of skeletal age at death based on the lateral-anterior sutures, *American Journal of Physical Anthropology* 68(1), 57–66.

Morales, V.B.
1983 Jarmo figurines and other clay objects with appendix: Notes on the textile and basketry impressions from Jarmo (J.M. Adovasio), in L.S. Braidwood, R.J. Braidwood, B. Howe, C.A. Reed. and P.J. Watson (eds.), *Prehistoric Archaeology along the Zagros Flanks*, Oriental Institute Publications 105, University of Chicago, Chicago.

Omori, T., Yamazaki, K., Itahashi, Y., Ozaki, H. and Yoneda, M.
2017 Development of a simple automated graphitization system for radiocarbon dating at the University of Tokyo, *The 14th International Conference on Accelerator Mass Spectrometry*.

Orange, D., Knittle, E., Farber, D. and Williams, Q.
1996 Raman spectroscopy of crude oils and hydrocarbon fluid inclusions: A feasibility study, in M.D. Dyer, C. McCammon and M.W. Schaefer (eds.), *Mineral Spectroscopy: A Tribute to Roger G. Burns*, The Geochemical Society Special Publication 5, The Geochemical Society, Washington, 65–81.

Pironon, J., Sawatzki, J. and Dubessy, J.
1991 NIR FT Raman microspectroscopy of fluid inclusions–Comparisons with Vis Raman and FT-IR microspectroscopies, *Geochimica et Cosmochimica Acta* 55, 3885–3891.

Reimer, P.J., Austin, W.E.N., Bard, E., Bayliss, A., Blackwell, P.G., Bronk Ramsey, C., Butzin, M., Cheng, H., Edwards, R.L., Friedrich, M., Grootes, P.M., Guilderson, T.P., Hajdas, I., Heaton, T.J., Hogg, A.G., Hughen, K.A., Kromer, B., Manning, S.W., Muscheler, R., Palmer, J.G., Pearson, C., J. van der Plicht, C., Reimer, R.W., Richards, D.A., Scott, E.M., Southon, J.R., Turney, C.S.M., Wacker, L., Adolphi, F., Büntgen, U., Capano, M., Fahrni, S.M., Fogtmann-Schulz, A., Friedrich, R., Köhler, P., Kudsk, S., Miyake, F., Olsen, J., Reinig, F., Sakamoto, M., Sookdeo, A. and Talamo, S.
2020 The IntCal20 Northern hemisphere radiocarbon age calibration curve (0–55 cal kBP), *Radiocarbon* 62(4), 725–757.

Sjøvold, T.
1990 Estimation of stature from long bones utilizing the line of organiccorrelation, *Human Evolution* 5, 431–447.

Schito, A., Romano, C., Corrado, S., Grigo, D. and Poe, B.
2017 Diagenetic thermal evolution of organic matter by Raman spectroscopy, *Organic Geochemistry* 106, 57–67.

Shoute, L., Schmidt, K., Hall, R., Webb, M., Rifai, S., Abel, P., Arboleda, P., Savage, A., Bulmer, J. and Loppnow, G.
2002 UV Raman spectroscopy of oilsands-derived bitumen and commercial petroleum products, *Applied Spectroscopy* 56, 1308–1313.

Trotter, M.
1970 Estimation of stature from intact long bones, in T.D. Stewart (ed.), *Personal Identification in Mass Disasters*, Smithsonian Institution Press Washington DC, 71–83.

Tsuneki, A., Rasheed, K., Watanabe, N., Anma, R. Tatsumi, Y. and Minami, M.
2019 Landscape and early farming at Neolithic sites in Slemani, Iraqi Kurdistan: A case study of Jarmo and Qalat Said Ahmadan, *Paléorient* 45/2, 33–51.

Tsuneki, A., Watanabe, N., Anma, R., Jammo, S., Saitoh, Y. and Saber, S.A.
2023 Preliminary report of the Charmo (Jarmo) prehistoric investigations, 2022, *al-Rāfidān* 46, 1–34 (published by the Institute for Cultural Studies of Ancient Iraq, in the School of Asia 21, Kokushikan University, Tokyo).

Tsuneki, A., Rasheed, K., Saber, S.A., Nishiyama, S., Anma, R., Ismail, B.B., Hasegawa, A., Tatsumi, Y., Miyauchi, Y., Jammo, S., Makino, M. and Kudo, Y.
2015 Excavations at Qalat Said Ahmadan, Slemani, Iraq-Kurdistan: First interim report (2014 season), *al-Rāfidān* 36, 1–50 (published by the Institute for Cultural Studies of Ancient Iraq, Kokushikan University, Tokyo).

Tsuneki, A., Rasheed, K., Saber, S.A., Nishiyama, S., Watanabe, N., Greenfield, T., Ismail, B.B., Tatsumi, Y. and Minami, M.
2016 Excavations at Qalat Said Ahmadan, Qaladizah, Iraq-Kurdistan: Second interim report (2015 season), *al-Rāfidān* 37, 89–142 (published by the Institute for Cultural Studies of Ancient Iraq, Kokushikan University, Tokyo).

Ubelaker, D.H.
1989 *Human Skeletal Remains: Excavation, Analysis, Interpretation*. Taraxacum, Washington DC.

de Vries, H. and Barendsen, G.W.
1954 Measurements of age by the carbon-14 technique, *Nature* 174, 1138–1141.

Zeidi, M., Riehl, S., Napierala, H. and Conard, N.J.
2012 Chogha Golan: A PPN site in the foothills of the Zagros Mountains, Ilam Province, Iran (Report on the first season of excavation in 2009), in R. Matthews, J. Curtis, M. Seymour, A. Fletcher, A. Gascoigne, C. Glatz, S.J. Simpson, H. Taylor, J. Tubb and R. Chapman (eds.), *Proceedings of the 7th International Congress on the Archaeology of the Ancient Near East. 12 April - 16 April 2010, the British Museum and UCL, London Volume 3 Fieldwork & Recent Research Posters*, Harrassowitz Verlag, Wiesbaden.

Zhang, N., Tian, Z., Leng, Y., Wang, H., Song, F. and Meng, J.
2007 Raman characteristics of hydrocarbon and hydrocarbon inclusions, *Science in China Series D: Earth Science* 50, 1171–1178.

Zhou, Q., Xiao, X., Pan, L. and Tiana, H.
2014 The relationship between micro-Raman spectral parameters and reflectance of solid bitumen, *International Journal of Coal Geology* 121, 19–25.